BORNEO SCIENCE
A JOURNAL OF SCIENCE AND TECHNOLOGY

BORNEO SCIENCE

A JOURNAL OF SCIENCE AND TECHNOLOGY

BORNEO SCIENCE
A JOURNAL OF SCIENCE AND TECHNOLOGY

ISSN 1394-4339

BORNEO SCIENCE

A JOURNAL OF SCIENCE AND TECHNOLOGY
JURNAL SAINS DAN TEKNOLOGI

September 2017

Volume 38 (Issue No.2)

CONTENT **Page**

ORIGINAL ARTICLES

A SHORT REVIEW OF ISOINDIGO ACCEPTOR FOR CONJUGATED POLYMERIC PHOTOVOLTAICS

Shu Er Tan, Wahidah Zabidi and Mohd Sani Sarjadi*

Faculty of Science and Natural Resources,
Universiti Malaysia Sabah,
Jalan UMS, 88400 Kota Kinabalu, Sabah, Malaysia.

*Corresponding author: msani@ums.edu.my

ABSTRACT. *This paper focussed on the recent development of conjugated polymers that contains isoindigo as acceptor moiety in the application of copolymeric solar cell. In the past decade, various modifications have been done either on the isoindigo acceptor itself or incorporated the isoindigo with different donor moieties. Recently, the power conversion efficiency (PCE) of this isoindigo-based polymeric photovoltaics have achieved up to ~7%. Hence, it is a promising acceptor for the photovoltaics and is expected to break through the recent PCE achievement in the future. This review briefly summarized the structures and properties of the isoindigo-based polymers that have been investigated by the past researches.*

KEYWORD. Isoindigo; Conjugated copolymers; Polymeric solar cells; Small molecules.

INTRODUCTION

Nowadays, energy is highly demanded in both industrial and domestic usages. Energy depletion issues are highly concerned by most developing countries. The non-renewable energy sources, e.g. fossil fuels, natural gas, petroleum, and etc., will soon be completely ware out in the near future. Hence, lots of researches have been done to improve the efficiency of energy harvesting from various renewable resources, e.g. biofuels, geothermal heat, hydroelectricity, wind energy, and solar energy. Amongst these non-renewable energies, photovoltaic cells are one of the promising alternatives which attract the attention of researchers. The photovoltaic cells have been applied in various types of commercial devices, e.g. light emitting diodes (OLEDs), field-effect transistors photodiodes, photo detectors, and solar cells. (Herzog *et al*., 2001; Rand *et al*., 2007; Darling & You, 2013; Liu *et al*., 2014; Zhang *et al*., 2015). In the 1900s, photovoltaic technology was limited to the application of aerospace, before the first oil crisis eruption in the early 1970s (Braga *et al.*, 2008). Solar energy is one of the promising renewable resources. Various types of photovoltaic solar cells have been invented to harvest the energy from the solar power. Among the existing solar cells, organic conjugated polymeric solar cells have been intensively studied and modified to improve the power conversion efficiency (PCE) (Wang *et al.*, 2014).

LITERATURE REVIEW

First and foremost, polyacetylene (PA) was found to possess excellent electrical conductivity in 1977 (Hideki *et al.,* 1977; Morin *et al.,* 2005). This breakthrough urged the study of the PA and other polymers in the application of electrical conducting materials. Unfortunately, the PA was insoluble in many organic solvents and relatively unstable than other polymer in the ambient condition. Because of these limitations, scientists encountered various difficulties during the fabrication of PA-based conducting materials (Rehahn *et al.,* 1989; Morin *et al.,* 2005). Besides PA, lots of polymers have been discovered as conjugated polymers, for example, poly(phenylene) (Rehahn *et al.,* 1989; Morin *et al.,* 2005), poly(*p*-phenylenevinylene)s (Burroughes *et al.,* 1990; Morin *et al.,* 2005), polythophenes (Leclerc & Faid, 1997; Leclerc, 1999; Morin *et al.,* 2005), polypyroles (Watanabe *et al.,* 1989; Morin *et al.,* 2005), polyaniline (D 'aprano *et al.,* 1992; Morin *et al.,* 2005), polyfluorenes (Neher, 2001; Morin *et al.,* 2005), and etc.

The active layer present in the photovoltaic solar cells have evolved from the initial silicon p-n junctions (Chapin *et al.,* 1954; Goetzberger & Hebling, 2000; Scharber *et al.,* 2006), single-component (Wohrle & Meissner, 1991; Cheng *et al.,* 2009), bilayer heterojunction (Tang, 1986; Sathiyan *et al.,* 2016), until the recent bulk heterojunction (Yu *et al.,* 1995; Zhou *et al.,* 2012) configuration. The solar energy is converted into electrical energy through the organic photovoltaic solar cells. The efficiency of this conversion can be assessed through the PCE value, which is a dependent variable that consist of three parameters, i.e. open circuit voltage (V_{oc}), short –circuit current density (J_{sc}) and fill factor (FF). The relationship between these factors could be expressed via the following maths equation in (1) (Günes *et al.,* 2007; Zhou *et al.,* 2012; Sathiyan *et al.,* 2016).

$$\text{PCE } (\eta_e) = \frac{V_{oc} \times I_{sc} \times FF}{P_{in}} \quad (1)$$

Over past decades, PCE of polymeric solar cells (PSCs) have been rapidly increased from 1% and eventually surpassed 10% (Cheng *et al.,* 2016). Various types of structural modifications have been done to improve the charge transport ability of the existing copolymers. A summary regarding the recent development of isoindigo-based copolymers with notable PCE value will be reported in the following section.

Isoindigo has been widely applied as the acceptor moiety along the polymeric backbone. It was found to have excellent electron withdrawing ability as it comprises two lactam rings (Stalder *et al.,* 2010; 2011; 2013, Sonar *et al.,* 2013; Wang *et al.,* 2014). The chemical structure of the isoindigo is illustrated in **Figure 1** (Estrada *et al.,* 2013). Recently, researchers have modified the isoindigo structure in various ways. One of these is that the benzene rings were replaced by five-membered thiophene rings and it was found that the polymer with thiophene substituted isoindigo possesses deep LUMO level which resulted

excellent ambipolar charge transport (Ashraf *et al.,* 2012; Dutta *et al.,* 2013). Besides that, 7,7'-diazaisoindigo was introduced in 2016, which the carbon located on the 7th and 7-th positions of isoindigo were replaced with nitrogen atoms (de Miguel *et al.,* 2016). This novel 7,7'-diazaisoindigo was found to have longer fluorescence lifetime than its isoindigo counterpart.

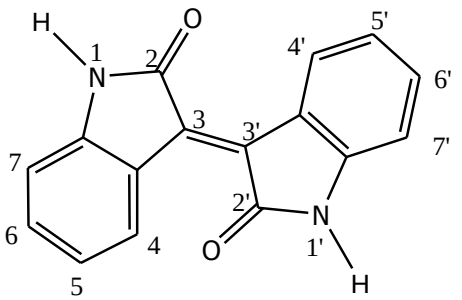

Figure 1 The isoindigo.

Isoindigo-Based Copolymers

The isoindigo monomer is normally synthesized with two bromine atoms located at its 6th and 6'th- positions. These bromine substituents are essential for the carbon-carbon coupling reaction with the chosen donor monomers to obtain the desire isoindigo-based polymers, as illustrated in **Figure 2**. Besides the Stille's protocol as shown in Figure 2 (Mei *et al.,* 2010), Suzuki's coupling reaction is also one of the pathways to polymerize the isoindigo with other monomers. However, the bromine substituents are required to convert to boron esters before carbon-carbon coupling reaction is carried out (Grenier *et al.,* 2012).

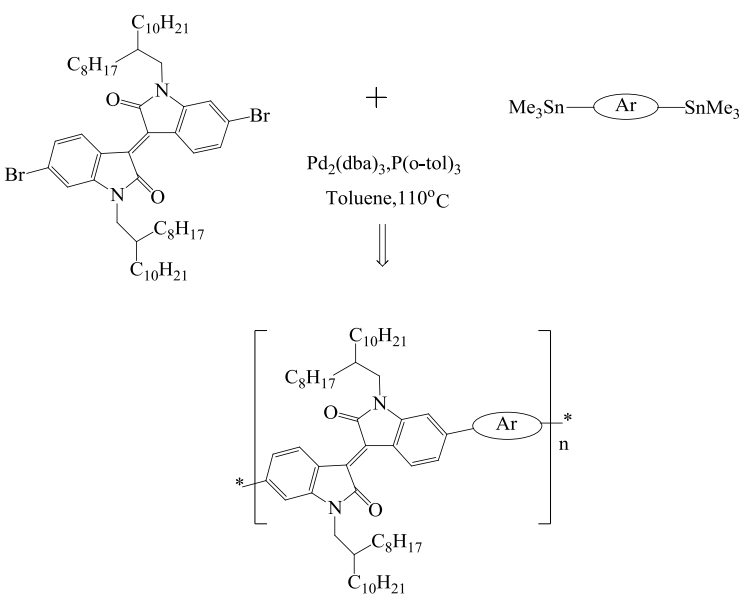

Figure 2: The Stille's protocol of the carbon-carbon coupling reaction.

Initially, the researchers incorporated the isoindigo acceptors with thiophene rings, i.e. **P1**-**P3**. Meanwhile, the influence of the N-alkyl chains which were located in the isoindigo was intensively studied. It was found that 2-hexyldecyl alkylated isoindigo-based copolymer **(P1)** shown best performance among the 2-ethylhexylated **(P2)** and 2-octyldodecylated **(P3)** isoindigo-based copolymer. **P1** possesses excellent thermal stability, while **P2** was found to be insoluble in common organic solvents. The PCE value obtained from P1-based copolymeric solar cell (PSC) is 3.0 %. For the **P3**, the PV performance is very low, c.a. 0.92 % PCE value. This is because the low hole mobility of the **P3**-based copolymer (Wang *et al.*, 2011a; Zhang *et al.*, 2011). Hence, the isoindigo monomers synthesized in the most of the later researches have applied the 2-hexyldecyl N-alkyl chains.

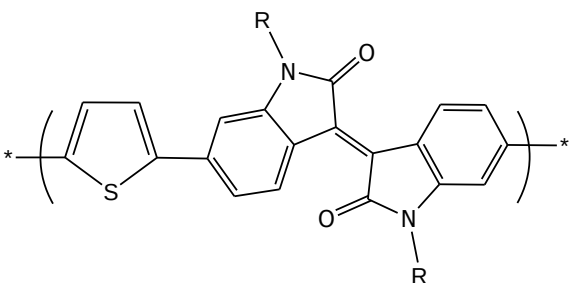

P1: R= 2-hexyldecyl

P2: R= 2-ethylhexyl

P3: R= 2-octyldodecyl

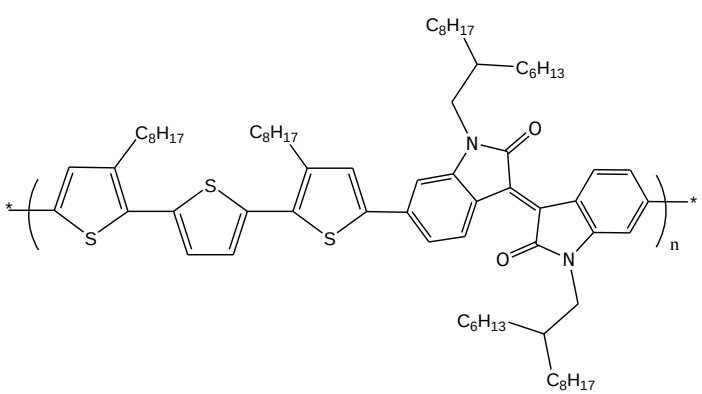

P4

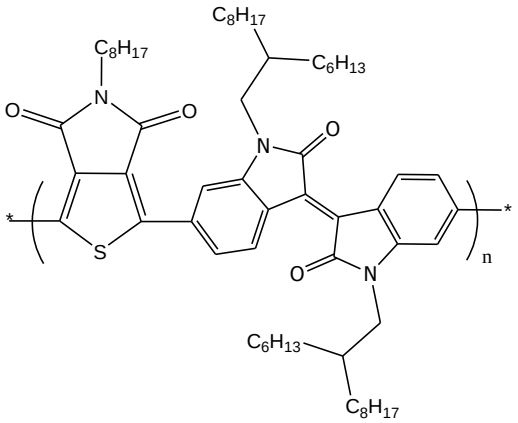

P5

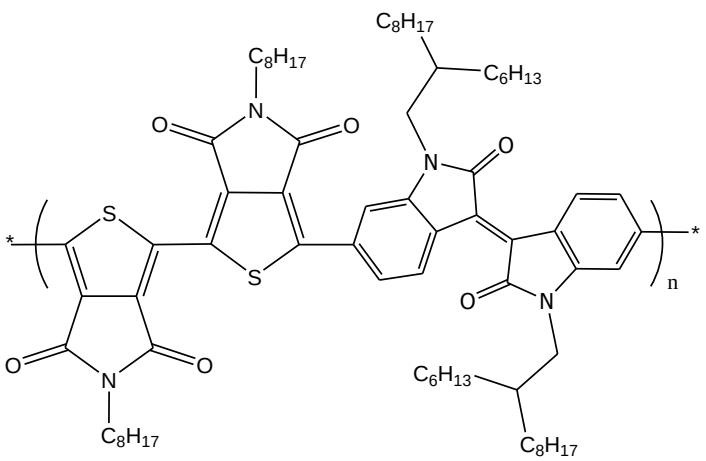

P6

In 2011, Wang and co-workers modified the donor moiety of P1-P3, by increasing the number of thiophene rings incorporated in between the isoindigo, i.e. **P4**. This has increased the conjugation length of the donor moieties. The PCE value has been improved up to 6.3% (Wang *et al.*, 2011b). During the past few years, various donors have been incorporated with isoindigo acceptors. One of the promising donor which has been used to polymerize with isoindigo is thieno [3,4-c]pyrrole-4,6-dione (BTD), for example the **P5** and **P6**. P5 consists of one BTD, while P6 comprises of two BTD for each donor-acceptor monomer. The results had shown that both P5 and P6 possess excellent electron mobility, i.e. 3.0 x 10^{-4} and 3.5 x 10^{-3} cm^2 s^{-1} V^{-1}, respectively (Grenier *et al.*, 2012). The details of P1-P6 have been summarized in **Table 1**. Furthermore, isoindigo have been intensively studied and incorporated with various types of donors to obtain PSC with excellent photovoltaic performance.

Table 1

Characteristics / Polymer	Copolymers						BHJ PSC								Ref.
	M_n [a] (kDa)	M_w [a] (kDa)	T_d [b] (^oC)	HOMO [c](eV)	LUMO [c] (eV)	PDI	E_g^{elec} [d](eV)	E_g^{opt} film [e](eV)	V_{OC} (V)	J_{SC} (mA/ cm^2)	FF	μ_h (cm^2/ Vs)	μ_e (cm^2/ Vs)	PCE (%)	
P1	n.a.	n.a.	400	-5.85	-3.88	2.2	1.97	1.60	0.89	5.4	0.63	n.a.	n.a.	3.0	(Wang *et al.*, 2011)
P2	Insoluble [No result]														(Zhang *et al.*, 2011)
P3	17.2	36.1	397	-5.49	-3.91	2.1	1.58	1.58	0.87	1.76	0.60	1.30×10^{-8}	n.a.	0.92	(Zhang *et al.*, 2011)
P4	n.a.	n.a.	380	-5.82	-3.83	n.a.	1.99	1.50	0.7	13.1	0.69	n.a.	n.a.	6.3	(Wang *et al.*, 2011)
P5	24	53	n.a.	-6.0	-4.2	2.2	1.8	1.72	n.a.	n.a.	n.a.	n.a.	3.0×10^{-4}	n.a.	(Grenier *et al.*, 2012)
P6	20	43	n.a.	-6.1	-4.2	2.2	1.9	1.75	n.a.	n.a.	n.a.	n.a.	3.5×10^{-3}	n.a.	(Grenier *et al.*, 2012)

[a] Measurement conducted by differential refractive index(DRI) detection. [b] Onset of degradation temperature obtained from TGA with 5% of weight loss. [c] HOMO and LUMO energy level determined from the onset of oxidation and reduction, respectively. [d] Electrochemical energy gap=l LUMO-HOMO l (eV). [e] Optical energy gap of the copolymeric thin film, E_g^{opt}. [f] μ_h represent hole mobility while μ_e represent electron mobility (cm^2/Vs).

CONCLUSION

Since isoindigo possesses excellent electron-withdrawing ability, it is a promising acceptor for the conjugated polymers in the application of organic photovoltaics. Various modifications on the chemical structure of the isoindigo still can be done in the future, to seek for a better isoindigo-based acceptor with promising properties.

LIST OF ABBREVATIONS

PCE = power conversion efficiency
PA = polyacetylene
V_{oc} = open circuit voltage
J_{sc} = short –circuit current density
FF = fill factor
HOMO = Higher Occupied Molecular Orbital
LUMO = Lower Unoccupied Molecular Orbital
BTD = thieno [3,4-c]pyrrole-4,6-dione

ACKNOWLEDGEMENT

This review was done in University Malaysia Sabah and financially supported by Fundamental Research Grant Scheme under FRG0413-SG-1/2015 grant.

REFERENCES

Ashraf, R. S., Kronemeijer, A. J., James, D. I., Sirringhaus, H., & McCulloch, I. (2012). A new thiophene substituted isoindigo based copolymer for high performance ambipolar transistors. *Chemical Communications*, *48*(33), 3939. https://doi.org/10.1039/c2cc30169e

Braga, A. F. B., Moreira, S. P., Zampieri, P. R., Bacchin, J. M. G., & Mei, P. R. (2008). New processes for the production of solar-grade polycrystalline silicon: A review. *Solar Energy Materials and Solar Cells*, *92*(4), 418–424. https://doi.org/10.1016/j.solmat.2007.10.003

Burroughes, J. H., Bradley, D. D. C., Brown, A. R., Marks, R. N., Mackay, K., Friend, R. H., Burns, P.L., & Holmes, A. B. (1990). Light-emitting diodes based on conjugated polymers. *Nature*. https://doi.org/10.1038/347539a0

Chapin, D. M., Fuller, C. S., & Pearson, G. L. (1954). A new silicon p-n junction photocell for converting solar radiation into electrical power [3]. *Journal of Applied Physics*, *25*(5), 676–677. https://doi.org/10.1063/1.1721711

Cheng, X., Wan, Q., Wu, Y., Guo, B., Guo, X., Li, Y., Zhang, M., Cui, C., & Li, Y. (2016). Toward high open-circuit voltage by smart chain engineering in 2D-conjugated polymer for polymer solar cells. *Solar Energy Materials and Solar Cells*. https://doi.org/10.1016/j.solmat.2016.01.017

Cheng, Y., Yang, S., & Hsu, C. (2009). Synthesis of Conjugated Polymers for Organic Solar Cell Applications. *Chemical Reviews*, *109*(11), 5868–5923. https://doi.org/10.1021/cr900182s

D ’aprano, G., Leclerc, M., & Zotti, G. (1992). Stabilization and Characterization of Pernigraniline Salt: The " Acid-Doped " Form of Fully Oxidized Polyanilines. *Macromolecules*. https://doi.org/10.1021/ma00034a013

Darling, S. B., & You, F. (2013). The case for organic photovoltaics. *RSC Adv.*, *3*, 17633–17648. https://doi.org/10.1039/c3ra42989j

de Miguel, G., Camacho, L., & García-Frutos, E. M. (2016). 7,7′-Diazaisoindigo: a novel building block for organic electronics. *J. Mater. Chem. C*, *4*(6), 1208–1214. https://doi.org/10.1039/C5TC03464G

Dutta, G. K., Han, A. R., Lee, J., Kim, Y., Oh, J. H., & Yang, C. (2013). Visible-near infrared absorbing polymers containing thienoisoindigo and electron-rich units for organic transistors with tunable polarity. *Advanced Functional Materials*, *23*(42), 5317–5325. https://doi.org/10.1002/adfm.201300536

Estrada, L. A., Stalder, R., Abboud, K. A., Risko, C., Bredas, J. L., & Reynolds, J. R. (2013). Understanding the electronic structure of isoindigo in conjugated systems: A combined theoretical and experimental approach. *Macromolecules*, *46*(22), 8832–8844. https://doi.org/10.1021/ma4013829

Goetzberger, A., & Hebling, C. (2000). Photovoltaic materials, past, present, future. *Solar Energy Materials and Solar Cells*, *62*(1), 1–19. https://doi.org/10.1016/S0927-0248(99)00131-2

Grenier, F., Berrouard, P., Pouliot, J.-R., Tseng, H.-R., Heeger, A. J., & Leclerc, M. (2012). Synthesis of new n-type isoindigo copolymers. *Polymer Chemistry*, *4*(6), 1836–1841. https://doi.org/10.1039/C2PY20986A

Günes, S., Neugebauer, H., & Sariciftci, N. S. (2007). Conjugated Polymer-Based Organic Solar Cells. *Chemical Reviews*, *107*(4), 1324–1338. https://doi.org/10.1021/cr050149z

Herzog, A. V., Lipman, T. E., & Kammen, D. M. (2001). Renewable energy sources. *Encyclopedia of Life* . Retrieved from http://rael.berkeley.edu/old_drupal/sites/default/files/old-site-files/2001/Herzog-Lipman-Kammen-RenewableEnergy-2001.pdf

Hideki, S., Louis, E. J., MacDiarmid, A. G., Chiang, C. K., & Heeger, A. J. (1977). Synthesis of Electrically-Conducting organic Polymers: Halogen Derivatives of Polyacatylene, (CH)x. *J.C.S., Chemical Communications*, (16), 1–5. https://doi.org/10.1039/c39770000578

Leclerc, M. (1999). Optical and electrochemical transducers based on functionalized conjugated polymers. *Advanced Materials*, *11*(18), 1491–1498. https://doi.org/10.1002/(SICI)1521-4095(199912)11:18<1491::AID-ADMA1491>3.0.CO;2-O

Leclerc, M., & Faid, K. (1997). Electrical and optical properties of Processable Polythiophene Derivatives: Structure-Property relationships. *Advanced Materials*, *9*(14), 1087–1094. https://doi.org/10.1002/adma.19970091404

Liu, Y., Zhao, J., Li, Z., Mu, C., Ma, W., Hu, H., Ade. H., & Yan, H. (2014). Aggregation and morphology control enables multiple cases of high-efficiency polymer solar cells. *Nature Communications*, *5:5293*(9), doi: 10.1038/ncomms6293. https://doi.org/10.1038/ncomms6293

Mei, J., Graham, K. R., Stalder, R., & Reynolds, J. R. (2010). Synthesis of Isoindigo-Based Oligothiophenes for Molecular Bulk Heterojunction Solar Cells. *Organic Letters*, *12*(4), 660–663. https://doi.org/10.1021/ol902512x

Morin, J.-F., Leclerc, M., Adès, D., & Siove, A. (2005). Polycarbazoles: 25 Years of Progress. *Macromolecular Rapid Communications*, *26*(10), 761–778. https://doi.org/10.1002/marc.200500096

Neher, D. (2001). Polyfluorene homopolymers: Conjugated liquid-crystalline polymers for bright blue emission and polarized electroluminescence. *Macromolecular Rapid Communications*. https://doi.org/10.1002/1521-3927(20011101)22:17<1365::AID-MARC1365>3.0.CO;2-B

Rand, B. P., Genoe, J., Heremans, P., & Poortmans, J. (2007). Solar Cells Utilizing Small Molecular Weight Organic Semiconductors. *Prog. Photovolt: Res. Appl.*, *15*(February 2013), 659–676. https://doi.org/10.1002/pip

Rehahn, M., Schlüter, A. D., Wegner, G., & Feast, W. J. (1989). Soluble poly(para-phenylene)s. 2. Improved synthesis of poly(para-2,5-di-n-hexylphenylene) via Pd-catalysed coupling of 4-bromo-2,5-di-n-hexylbenzeneboronic acid. *Polymer*. https://doi.org/10.1016/0032-3861(89)90079-7

Sathiyan, G., Sivakumar, E. K. T., Ganesamoorthy, R., Thangamuthu, R., & Sakthivel, P. (2016). Review of carbazole based conjugated molecules for highly efficient organic solar cell application. *Tetrahedron Letters*, *57*(3), 243–252. https://doi.org/10.1016/j.tetlet.2015.12.057

Scharber, M. C., Mühlbacher, D., Koppe, M., Denk, P., Waldauf, C., Heeger, A. J., & Brabec, C. J. (2006). Design rules for donors in bulk-heterojunction solar cells - Towards 10 % energy-conversion efficiency. *Advanced Materials*, *18*(6), 789–794. https://doi.org/10.1002/adma.200501717

Sonar, P., Tan, H.-S., Sun, S., Lam, Y. M., & Dodabalapur, A. (2013). Isoindigo dye incorporated copolymers with naphthalene and anthracene: promising materials for stable organic field effect transistors. *Polymer Chemistry*, *4*(6), 1983. https://doi.org/10.1039/c2py20942j

Stalder, R., Mei, J., Graham, K. R., Estrada, L. a, & Reynolds, J. R. (2013). Isoindigo, a Versatile Electron-Deficient Unit For High-Performance Organic Electronics. *Chemistry of Materials*, *26*(1), 664–678. https://doi.org/10.1021/cm402219v

Stalder, R., Mei, J., & Reynolds, J. R. (2010). Isoindigo-based donor-acceptor conjugated polymers. *Macromolecules*, *43*(20), 8348–8352. https://doi.org/10.1021/ma1018445

Stalder, R., Mei, J., Subbiah, J., Grand, C., Estrada, L. A., So, F., & Reynolds, J. R. (2011). n-Type Conjugated Polyisoindigos. *Macromolecules*, *44*(16), 6303–6310. https://doi.org/10.1021/ma2012706

Tang, W. C. (1986). Two-layer Organic Photovoltaic Cell, *48*(2), 183–185.

Wang, E., Ma, Z., Zhang, Z., Henriksson, P., Inganäs, O., Zhang, F., & Andersson, M. R. (2011a). An isoindigo-based low band gap polymer for efficient polymer solar cells with high photo-voltage. *Chemical Communications*, *47*(17), 4908. https://doi.org/10.1039/c1cc11053e

Wang, E., Ma, Z., Zhang, Z., Vandewal, K., Henriksson, P., Inganäs, O., Zhang, F. & Andersson, M. R. (2011b). An Easily Accessible Isoindigo-Based Polymer for High-Performance Polymer Solar Cells. *Journal of the American Chemical Society*, *133*(36), 14244–7. https://doi.org/10.1021/ja206610u

Wang, E., Mammo, W., & Andersson, M. R. (2014). 25th anniversary article: Isoindigo-based polymers and small molecules for bulk heterojunction solar cells and field effect transistors. *Advanced Materials*, *26*(12), 1801–1826. https://doi.org/10.1002/adma.201304945

Watanabe, A., Murakami, S., Mori, K., & Kashiwaba, Y. (1989). Electronic properties of polypyrrole/n-Si heterojunctions and polypyrrole/metal contacts. *Macromolecules*, *22*(11), 4231–4235. https://doi.org/10.1021/ma00201a016

Wohrle, B. D., & Meissner, D. (1991). Organic Solar Cells, *3*, 129–138.

Yu, G., Gao, J., Hummelen, J. C., Wudl, F., & Heeger, A. J. (1995). Polymer Photovoltaic Cells - Enhanced Efficiencies Via a Network of Internal Donor-Acceptor Heterojunctions. *Science*, *270*(5243), 1789–1791. https://doi.org/10.1126/science.270.5243.1789

Zhang, G., Fu, Y., Xie, Z., & Zhang, Q. (2011). Synthesis and Photovoltaic Properties of New Low Bandgap Isoindigo-Based Conjugated Polymers. *Macromolecules*, *44*(6), 1414–1420. https://doi.org/10.1021/ma102357b

Zhang, S., Ye, L., Zhao, W., Yang, B., Wang, Q., & Hou, J. (2015). Realizing over 10% efficiency in polymer solar cell by device optimization. *Science China Chemistry*, *58*(2), 248–256. https://doi.org/10.1007/s11426-014-5273-x

Zhou, H., Yang, L., & You, W. (2012). Rational Design of High Performance Conjugated Polymers for Organic Solar Cells. *Macromolecules*, *45*(2), 607–632. https://doi.org/10.1021/ma201648t

CHARACTERIZATION OF DIFFERENT METAL OXIDE PROMOTED ALUMINA CATALYST

S.M. Anisuzzaman[a,b,*], Awang Bono[b], Duduku Krishnaiah[b], F. A. Lahin[b], C. Ramlan[b]

[a]Energy Research Unit (ERU),
[b]Chemical Engineering Programme, Faculty of Engineering,
Universiti Malaysia Sabah, 88400 Kota Kinabalu, Sabah, MALAYSIA.

[*]Correspondence author. Tel: +6088-320000 ext. 3222, Fax: +6088-320348,
E-mail address: anis_zaman@ums.edu.my; dr.anis.ums@gmail.com

ABSTRACT. *In this study, different metal oxide alumina promoted catalysts were prepared and characterized. All the catalysts (CaO/Al_2O_3, CuO/Al_2O_3, FeO/Al_2O_3, MnO/Al_2O_3, NiO/Al_2O_3 and ZnO/Al_2O_3) were prepared using the incipient wetness impregnation method followed by drying and calcination. The characterization of all six samples of catalysts was done to determine the surface morphology, porosity, functional group, thermal stability, metal content and particle size distribution. Scanning electron microscope (SEM) analysis of samples showed that there were pores on the surface of the alumina. Mercury intrusion porosimetry (MIP) showed that copper oxide alumina promoted (CuO/Al_2O_3) had the high porosity which is 36.77 m^2/g followed by zinc oxide (ZnO/Al_2O_3), calcium oxide (CaO/Al_2O_3) nickel oxide (NiO/Al_2O_3) manganese oxide (MnO/Al_2O_3) and ferric oxide alumina promoted (FeO/Al_2O_3) catalysts. Fourier transform infrared spectroscopy (FTIR) analysis showed the presence of by-product existed in all catalysts. Atomic absorption spectroscopy (AAS) analysis showed the presence of Cu, Fe and Zn in the CuO/Al_2O_3, FeO/Al_2O_3 and ZnO/Al_2O_3, while Ca was absent in CaO/Al_2O_3. Besides, through thermo-gravimetric analyzer (TGA) and differential thermal analysis (DTA), all the catalysts showed a slight decrease in weight which can be considered as a stable catalyst. The particle size distribution analysis using the Zetasizer showed the particle size mean based on the intensity of CaO/Al_2O_3, CuO/Al_2O_3, FeO/Al_2O_3, MnO/Al_2O_3, NiO/Al_2O_3 and ZnO/Al_2O_3 were 2305 nm, 5560 nm, 5560 nm, 1281 nm, 1281 nm and 3580 nm, respectively.*

KEYWORDS. Biofuel, metal oxide promoted alumina catalyst, wet incipient impregnation method

INTRODUCTION

Fossil fuels are the main source of energy worldwide. The nature of fossil fuels is unsustainable and their cost is rapidly increasing. Besides that, fossil fuels have huge environmental impact including greenhouse effect which cause global warming and climate change (Aliyu *et al.*, 2014; Dorado *et al.*, 2003). An alternative and renewable energy source such as biomass has been developed in order to decrease the dependence on fossil fuels and reduce the carbon dioxide (CO_2) emissions (Gan and Li, 2008; Hashim and Ho, 2011). Even though the generation of energy out of this fuel releases CO_2, it is in fact much lower compared to the CO_2 emissions from fossil fuels. Besides, the CO_2 release from the biomass is available to produce a new biomass via photosynthesis process where the CO_2 in the air react with water and sunlight to produce carbohydrates that form the building blocks of biomass (McKendry, 2002).

In order to make use of the biomass energy potential, several conversion methods can be applied including biochemical and thermochemical conversion. In biochemical conversion processes, basically the biomass or biomass-derived compounds will be converted into desirable products with the presence of enzymes and microorganisms as the biocatalysts. This process produces a small number of discrete products in high yield using biological catalysts (Bridgwater, 2011). In thermochemical conversion, there are three main thermal processes available including pyrolysis, gasification and combustion.

Like biochemical conversion, thermochemical conversion can also be done with and without the presence of catalyst. Catalyst accelerates a chemical reaction without affecting the position of the equilibrium (Hagen, 2006). It increases the rate of a reaction without modifying the overall standard Gibbs energy change in the reaction. A variety of metal oxide promoted alumina catalyst was synthesized using the incipient wetness impregnation method. Impregnation is contacting a solid with a liquid containing the components to be deposited on the surface (Haber *et al.*, 1995).

In this study, six types of metal oxide alumina promoted catalysts were prepared and characterized accordingly. All of these catalysts were characterized using scanning electron microscope (SEM), mercury intrusion porosimetry (MIP), fourier transform infrared spectroscopy (FTIR), atomic adsorption spectrophotometer (AAS), thermal gravimetric analysis (TGA) and Zetasizer. Impregnation method which was chosen in this study was contacted with a certain amount of solution of the metal precursor followed by drying and calcination. Table 1 summarized the previous studies of different metal oxide catalysts preparation

Table 1: Previous studies of different metal oxide catalysts preparation

Reference	Impregnation method	Drying method	Calcination method
Huang *et al.*, 2005	γ-Al_2O_3 was ground to 150-250 µm particles. The appropriate amount of metal nitrate, $(Zn(NO_3)_2.6H_2O)$, dissolved in distilled water to form an aqueous solution. The solution was added dropwise to γ-Al_2O_3 particles and the solid was shaken for 10 min to ensure uniform distribution of the solution.	The wet solid was dried in air (90°C, 16 hours)	The catalyst precursors were calcined at 500°C for 3 hours in static air, at the temperature ramp rate of 10°C/ min
Bakar *et al.*, 2009	$Ni(NO_3)_2.6H_2O$ was dissolved with minimum amount of distilled water. Mixed catalysts solution was prepared by mixing appropriate amount of metal nitrate salts. Wet impregnation method was used to prepare Al_2O_3 supported catalyst by impregnating the catalyst solution on Al_2O_3 beads support for 15 min.	Dried at 80°C for 24 hours	Calcined in air at 400°C for 5 hours
Kiss *et al.*, 2012	Spinels of Zn, Mg and Cu were synthesized by impregnation of alumina or their precursors, with the corresponding metal salts, $Zn(NO_3)_2.6H_2O$ and $Cu(NO_3)_2.3H_2O$ in aqueous solution.	The impregnation sample precursors were dried at 105 °C overnight.	Calcined at 350°C for 4 hours in air
Buitrago-Sierra *et al.*, 2012	The alumina was calcined at 500°C for 5 hours. The ZnO-modified alumina support were prepared by impregnating the γ-Al_2O_3 with an aqueous solution of $Zn(NO_3)_2.6H_2O$. The slurry formed was stirred at room temperature for 12 hours and the excess solvent was removed by heating at 80°C under vacuum in a rotary evaporator.	The solids were dried overnight at 100°C	Calcined at 700°C for 4 hours at a heating rate of 2 K min^{-1}
Rosal *et al.*, 2010	The MnO_x/Al_2O_3 catalyst was prepared by incipient wetness impregnation dried γ-Al_2O_3 using an aqueous solution of $Mn(CH_3COO)_2.4H_2O$.	Dried in air at 150°C	Calcined at 500°C for 3 hours
Zabeti *et al.*, 2009	8 g of γ-alumina in powder form was preheated at 600°C for 1 hour to remove physisorbed water. For each catalyst, a desired amount of precursor was dissolved in 50 mL of distilled water and introduced onto the alumina in a glass flask; the mixture was stirred for 4 hours at room temperature.	The obtained precipitation was heated overnight in an oven in order to remove water through evaporation.	All catalysts were calcined in air at desired temperature for 5 hours.
Zabeti *et al.*, 2010	The CaO/Al_2O_3 catalyst was prepared using optimum condition, calcium acetate with a mass ratio of 1:1 to the support was dissolved in 50 mL of distilled water and stirred with 40 g alumina at room temperature for 4 hr.	The obtained slurry was heated up at 100°C in an oven overnight in order to remove the water.	Catalyst was calcined in air at 718°C for 5 hours using a muffle furnace.

MATERIALS & METHODS

Materials

The activated alumina was obtained from Edwards High Vacuum Int. In this study, a total of six metal nitrate were used, one of the metal nitrate was calcium nitrate tetrahydrate [$Ca(NO_3)_2.4H_2O$], in crystalline form, and it was obtained from R & M Marketing, Essex, U.K, while the rest, copper (II) nitrate trihydrate, $Cu(NO_3)_2.3H_2O$; ferric (III) nitrate nonahydrate, $Fe(NO_3)_3.9H_2O$; nickel (II) nitrate hexahydrate, $Ni(NO_3)_2.6H_2O$; manganese (II) nitrate tetrahydrate, $Mn(NO_3)_2.4H_2O$; zinc nitrate hexahydrate, $Zn(NO_3)_2.6H_2O$ were in liquid form, and all of these metal nitrates were obtained from Scharlab S.L. The mass for each metal solution varied from one another since each metal have their own properties that affect the molarity of solution formed. By following Hongmei method, molarity of 0.2M is fixed for each solution. By using this molarity, the mass and volume for each metal used was calculated accordingly.

Incipient wetness impregnation

All the metal oxide promoted alumina catalysts were prepared using the incipient wetness impregnation method followed by drying and calcination. The alumina was first calcined for 1 hour at 600^oC before used so that the physisorbed water can be removed. An appropriate amount of metal nitrate, $Ca(NO_3)_2.4H_2O$, $Fe(NO_3)_3.9H_2O$, $Zn(NO_3)_2.6H_2O$, $Ni(NO_3)_2.6H_2O$, $Cu(NO_3)_2.3H_2O$ and $Mn(NO_3)_2.4H_2O$, were dissolved in distilled water (0.9 mL) to form an aqueous solution. Then, the aqueous solution was introduced into 1 g of the alumina and stirred at room temperature for 4 hours. The obtained slurry was dried at 120^oC for 18 hours and calcined in nitrogen gas by using tube furnace as shown in Figure 1 at 500^oC for 5 hours. Catalyst was then kept in desiccator with the presence of silica and KOH pellets in order to avoid water and CO_2 contact with the catalyst (Zabeti *et al.*, 2009; Zabeti *et al.*, 2010; Buitrago-Sierra *et al.*, 2012). Figure 1 showed the experimental set up for the metal oxide catalysts preparation.

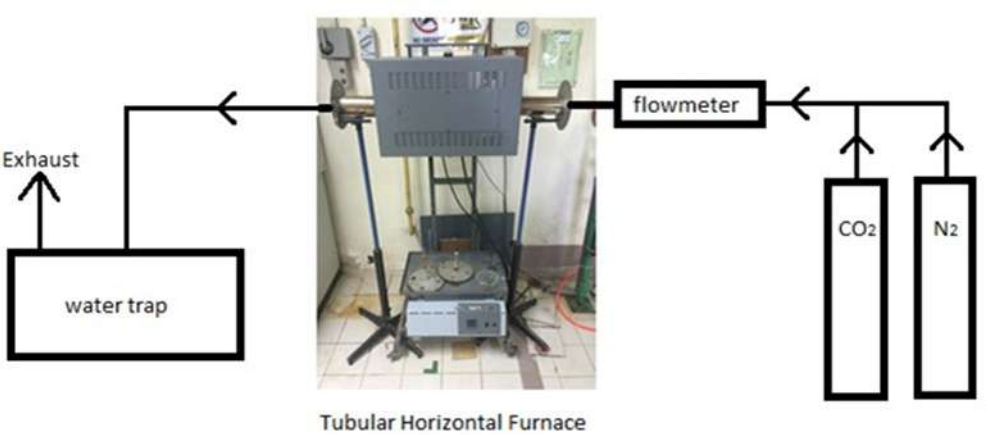

Figure 1: Experimental set up for the metal oxide catalysts preparation

Characterization of metal oxide promoted alumina catalyst

The characterization of all six samples was carried out in order to determine the functional group present in the catalyst, thermal stability of the catalyst, surface morphology, surface area and porosity, metal content and particle size distribution of the catalysts.

Surface morphology

The surface morphology of metal oxide promoted alumina catalyst was done by using scanning electron microscope (SEM) Carl Zeiss Model MA10. The instrument set up were as follow; vacuum mode = variable pressure, magnifications = 1000x, and signal VPSE G3 was chosen for non-conductive sample.

Surface area and porosity

The analysis in determining the surface area and total porosity of the metal oxide promoted alumina catalyst was done by using mercury intrusion porosimetry (MIP) of Thermo Electron Corporation (Pascal 440 Series). Mercury porosimetry technique is useful method to investigate the porous structure by giving reliable information such as pore size/volume distribution, particle size distribution, bulk density and specific surface area. About 0.80 g ± 0.05 of sample was prepared and inserted into a dilatometer. Dilatometer was then placed into the mercury preparation machine. Before the mercury was purged into the dilatometer, vacuum was applied for 5 minutes. After that, mercury was filled slowly until it reached the half of the dilatometer. Then, the air was purged slowly to prevent any bubbles in the dilatometer. After that, the air was stopped and the vacuum was applied again for 5 minutes. Next, the mercury was filled until it reached the line mark at the tube that was attached to the dilatometer. The dilatometer was brought out and some oil was put after the line mark. The mercury was weighed using a mass balance. Finally, the dilatometer was placed in the porosimetry machine for analysis.

Functional group

The analysis of functional group was done using Cary 630 FTIR, Agilent Technologies and the name of method used was Betullin ATR 030714. Initially, the sample holder was cleaned by using propan-2-ol and kimwipes tissue to prevent the new samples that were analyzed from being contaminated. A small amount of sample (~1 g) was placed on the sample holder. The FTIR was set to scan in the range of 650 cm^{-1} to 4000 cm^{-1}. After obtaining the results, the data was saved as ASCII file and then used to plot a graph in Microsoft Excel.

Metal element

The analysis of metal element contained in the catalysts samples were done by using Z-5000 Polarized Zeeman atomic absorbance spectrophotometer (AAS). To analyze the sample, it must be in liquid form. In order to convert the powder catalyst to liquid, the digest method was followed and standard solution for each sample was prepared.

Thermal stability

The thermal stability of catalysts samples were analyzed by using TGA 6 Thermo-Gravimetric Analyzer (Perkin Almer). There are two analyses done which was thermal gravimetric analysis (TGA) and differential thermal analysis (DTA). TGA was used to determine a material's thermal stability and its fraction of volatile components by monitoring the weight change that occurs as a specimen is heated. The measurement is normally carried out in air or in an inert atmosphere, and the weight is recorded as a function of increasing temperature, some instruments also record the temperature difference between the specimen and one or more reference pans (differential thermal analysis, DTA).About 15 .0 mg ± 0.5 of samples were measured and placed in the sample holder in the instrument. The operating condition of the analysis was done at 50 to 1000^{o}C, ramped at 30^{o}C/min under the presence of nitrogen gas which flow was set at 100 mL/min. The collection of information on the decomposition of the sample was then interpreted based on the data obtained for TGA and DTA.

Particle size

The particle size distribution of the samples was done by using Malvern Zetasizer Nano Series Instrument with water as a dispersant with refractive index of 1.330. Initially, 0.5 g of each sample was prepared and placed in the beaker. After that, 20 mL of distilled water was poured into the beaker and mixed with the sample. The mixture was left to sediment for 24 hours before it can be pipetted. After the solution was pipetted, it was inserted to a specific cuvette of the instrument with minimum sample volume of 15µm.

RESULTS & DISCUSSION

SEM analysis

The SEM images of the alumina were shown in Figure 2 with the magnification of 1000x which operated at 15 kV. Based on the Figure 2, it showed that the alumina support showed uniform roughness at the surface with granular structure and had pores on the surface. Pores on the surface of the alumina were important because the pores would be introduced to the metal oxide catalyst by using impregnation method.

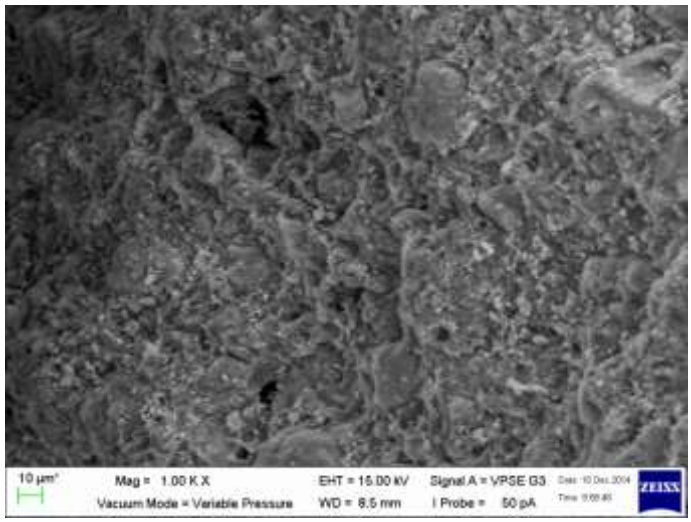

Figure 2: SEM micrographs (x1000 magnification) of alumina

Surface area and porosity

The activity of the catalytic system usually related to its textural properties, particularly, the specific surface area and the crystallite size. On account of this, the surface area and porosity of the alumina and metal oxide catalysts promoted alumina was done by using MIP. The results were shown in Table 2.

Table 2: Data of porosimetry for alumina and metal oxide promoted alumina catalyst

Samples	Total specific surface area, m^2/g	Total porosity (%)	Average pore diameter (nm)	Total cumulative volume (mm^3/g)
Alumina	17.59	14.21	25.83	173.33
ZnO/Al_2O_3	22.07	36.14	37.81	246.81
CaO/Al_2O_3	23.84	32.60	20.88	242.63
MnO/Al_2O_3	24.78	18.08	59.37	262.22
CuO/Al_2O_3	26.14	36.77	34.82	271.08
FeO/Al_2O_3	26.72	16.01	53.67	290.00
NiO/Al_2O_3	28.55	23.18	29.53	308.54

Based on Table 2, all the metal oxide promoted alumina catalysts exhibited low specific surface areas ranging from 22.07 to 28.55 m^2/g. NiO/Al_2O_3 had the highest surface area within the catalysts. While ZnO/Al_2O_3 showed the smallest surface area However, it could be observed that the specific surface area of the metal oxide promoted alumina catalysts were bigger than the area of the alumina support. It could be assumed that the impregnation method used did not cause any blockage of the support pores.

According to Nascimento *et al.*, (2011), blockage will only occur when there was too long contact time between the support and the solution used for the impregnation in order to perform the ion exchange. High total porosity was shown by CuO/Al_2O_3 and ZnO/Al_2O_3 which were 36.77% and 36.14% respectively, while FeO/Al_2O_3 had the lowest total porosity of 16.01%. Large surface area and high porosity would increase the rate of reaction. Large surface area allowed the penetration through the catalyst and therefore making it became easier , meanwhile high porosity allowed more molecule to molecule collision occur which also known as molecular diffusion. The largest pore diameter was recorded by MnO/Al_2O_3 followed by FeO/Al_2O_3 which were about 59.37 nm and 53.67 nm respectively. CaO/Al_2O_3 showed the smallest pore diameter of 20.88 nm and it was even smaller than the alumina support which was 25.83 nm. The total cumulative volumes for all metal oxide catalysts were recorded higher than the cumulative volume of the alumina support where NiO/Al_2O_3 stated the highest value of 308.54 mm^3/g. The increasing cumulative volume of the alumina support might be due to its non-affected structure which meant that there was no shrinkage or broken bonds within the alumina structure during the impregnation process (Pua *et al.*, 2011).

FTIR analysis

The results of the analysis functional group of metal oxide promoted alumina catalyst were as shown in Figure 3.

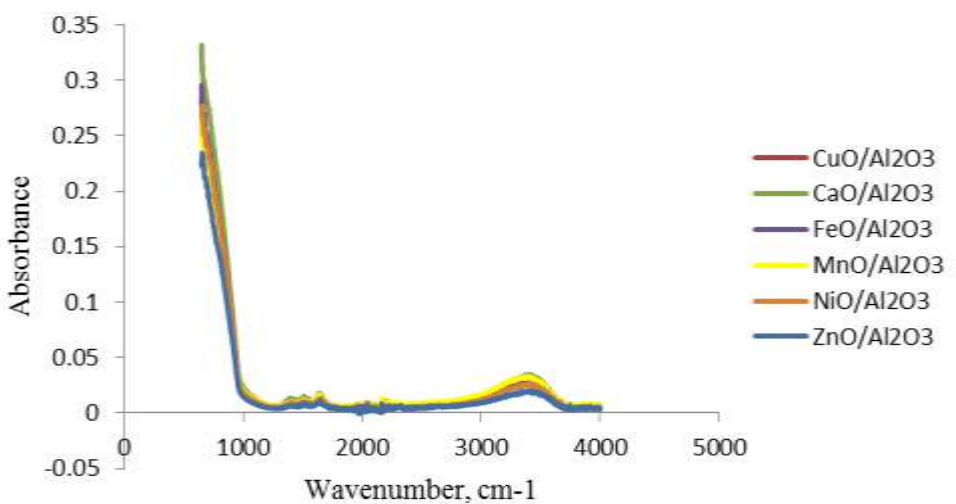

Figure 3: FTIR Spectra for CuO/Al_2O_3, CaO/Al_2O_3, FeO/Al_2O_3, MnO/Al_2O_3, NiO/Al_2O_3, ZnO/Al_2O_3

Based on Figure 3, it could be observed that all metal oxide promoted alumina catalysts had similar wavenumber. Based on Li (2005), the absorption bands at 1350 to 1500 cm^{-1} associated with the CH_3 deformation mode and the CH_2 scissor mode. While, absorption

band at 1635 cm^{-1} assigned to the C=C stretching mode. Absorption due to C-H stretching modes between 3100 to 3000 cm^{-1} were also observed even the peak could occur in a very small range. Plus, absorption bands at 1688 and 1709 cm^{-1} were assigned to C=O stretching mode of the COOH group. However, all of these were possibly due to the by-products, since all the metal oxide promoted alumina catalyst were heavy metals and may not contain any functional group.

Elemental compositions

The metal oxide promoted alumina catalysts had been analyzed by using atomic absorption spectrophotometer to determine the selected elements that might exist in the samples. The results were shown in Table 3.

Table 3: Concentration (ppm) of metal elements in catalyst samples

Samples	Concentration (ppm)			
	Ca	Cu	Fe	Zn
CaO/Al_2O_3	-0.037	-	-	-
CuO/Al_2O_3	-	1.577	-	-
FeO/Al_2O_3	-	-	1.922	-
ZnO/Al_2O_3	-	-	-	1.491

From Table 3, it could be seen that only CaO/Al_2O_3 obtained a negative value for the concentration which meant that there was no calcium element present in the catalyst. This might be due to the time taken for the impregnation method for CaO/Al_2O_3. The $Ca(NO_3)_2.4H_2O$ was in crystalline form and when it dissolved in 0.9 mL of distilled water, the solution that was formed was very little quantity in which it only can be stirred manually with the alumina instead of using the hot plate. It took 10 minutes for the impregnation of CaO/Al_2O_3 which was really short compared to the impregnation time for other catalysts which was approximately 4 hours. This was mainly because there was no ion exchange occurrence between the $Ca(NO_3)_2.4H_2O$ and alumina due to the very short time taken for impregnation.

Thermal gravimetric analysis

Based on the TGA, there were two analyses done in the same time which are TGA and DTA. TGA provided information about the percentage weight loss of the sample and DTA analyzed the decomposition of the functional group in the sample per unit time. Figure 4 and Figure 5 showed the sample results of CaO/Al_2O_3 for TGA and DTA respectively.

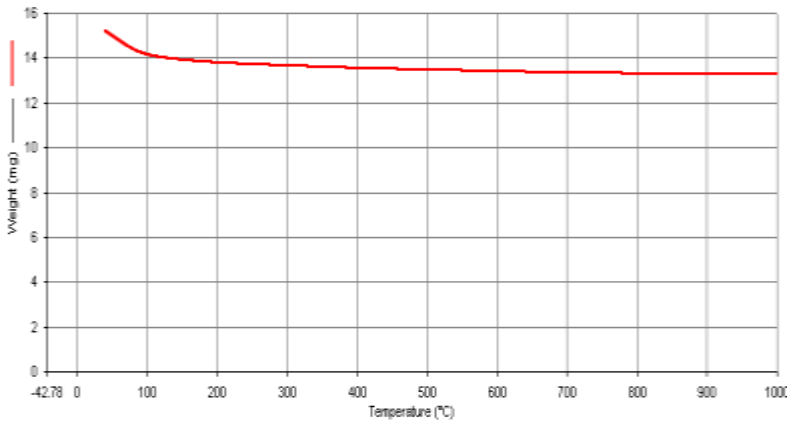

Figure 4: Thermal gravimetric analysis (TGA) of CaO/Al_2O_3

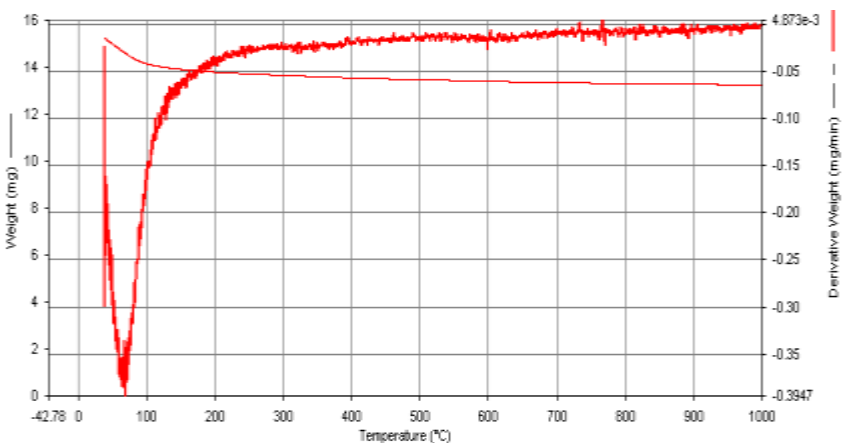

Figure 5: Derivative thermal analysis (DTA) of CaO/Al_2O_3

Based on the result of TGA, it could be observed that the CaO/Al_2O_3 showed only a slight decrease in weight up to 100°C. Generally, all the metal oxide promoted alumina catalyst had shown the same results, it could be observed that there was no change except for the weight loss that corresponded to liberation of adsorbed moisture between room temperature and 100°C (Ookawa 2012). Besides that, no other losses were recorded in the temperature range of 150 to 1000°C. It was because the temperature from 0 to 800°C was basically to measure the organic burning. Since all of the samples were in metal oxide state, not organic, it would be burnt at the temperature of 1500°C and above. However, the available analyzer could only reach the burning temperature of a maximum of 1000°C. The final weights (mg) of CaO/ Al_2O_3, CuO/ Al_2O_3, FeO/ Al_2O_3, MnO/ Al_2O_3, NiO/ Al_2O_3 and ZnO/ Al_2O_3 up to 1000°C were 13.26 mg, 14.50 mg, 13.30 mg, 14.08 mg, 13.56 mg and 13.96 mg, respectively. On the other hand, the decomposition of moisture could be seen clearly in DTA (in mg/min) as shown in Figure 5, which was interconnected with TGA analysis, between 30 to 100°C.

Particle size distribution

The particle size distribution was analyzed by using the Zetasizer in determining the size of the particle of metal oxide promoted alumina catalysts. The result of particle size distribution by intensity of metal oxide promoted alumina catalyst was shown in Figure 6.

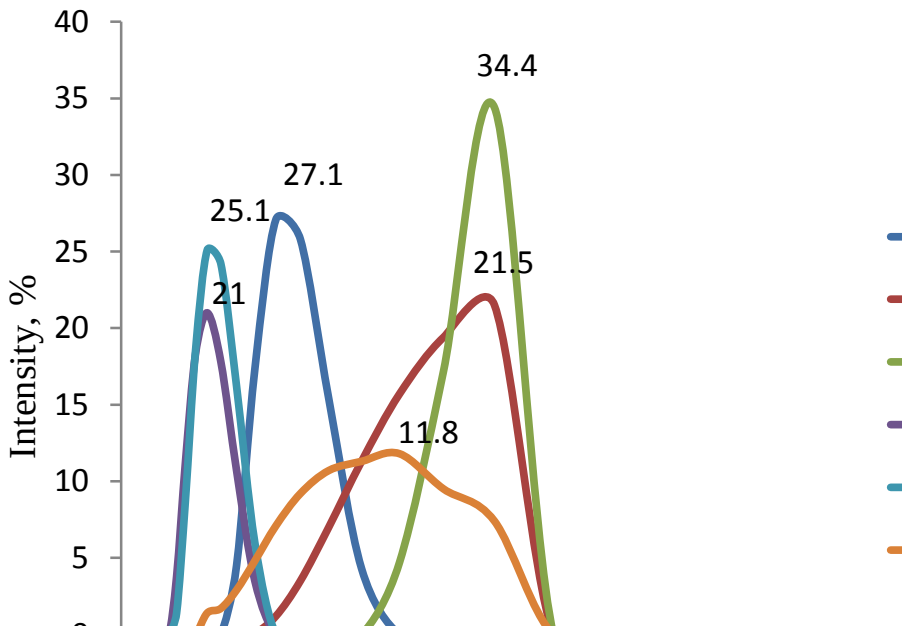

Figure 6: Particle size distribution based on intensity for metal oxide promoted alumina catalyst

Based on Figure 4, the particle size distribution by intensity of Cu/Al_2O_3 and FeO/Al_2O_3 stated the larger particle size of 5560 nm. Whereas NiO/Al_2O_3 and MnO/Al_2O_3 recorded the smallest particle size which was 1281 nm. It could be observed that NiO/Al_2O_3, CaO/Al_2O_3, MnO/Al_2O_3 and FeO/Al_2O_3 showed a normal continuous distribution graph which was a bell shaped graph. However, for CuO/Al_2O_3 and ZnO/Al_2O_3, the shape of the graph was slightly different. This might be due to the inconsistent data values obtained during the analysis. The particle size distribution analysis showed the particle size mean based on intensity of CaO/Al_2O_3, CuO/Al_2O_3, FeO/Al_2O_3, MnO/Al_2O_3, NiO/Al_2O_3 and ZnO/Al_2O_3 were 2305 nm, 5560 nm, 5560 nm, 1281 nm, 1281 nm and 3580 nm, respectively.

CONCLUSION

Based on the AAS analysis, from four metal oxides promoted alumina catalysts that were analyzed, only metal content of Cu, Fe and Zn were present in CuO/Al_2O_3, FeO/Al_2O_3 and ZnO/Al_2O_3 meanwhile Ca element was absent in CaO/Al_2O_3. Throughout the TGA and DTA analysis, above the temperature of 100^oC all catalyst samples showed a stable result. Furthermore, alumina support that was analyzed by using SEM was observed to have pores on the surface which could be introduced to the metal solution for impregnation method. On the other hand, the automated mercury porosimetry analysis showed that CaO/Al_2O_3, CuO/Al_2O_3 and ZnO/Al_2O_3 had high total porosity (%). Based on results from Zetasizer, all the catalyst samples demonstrated different particle sizes in the range of 800-6500 nm based on their intensity.

REFERENCES

Aliyu, A. S., Ramli, A. T.,Saleh, M. A. 2014. Environmental impact assessment of a new nuclear power plant (NPP) based on atmospheric dispersion modeling. *Stochastic Environmental Research and Risk Assessment* 28 (7): 1897-1911.

Bakar, W. A.W. A., Othman, M.Y., Ali, R. Yong, C.K., Toemen, S. 2009. The investigation of active sites on nickel oxide based catalysts towards the in-situ reactions of methanation and desulfurization. *Modern Applied Science* 3(2): 35-43.

Bridgwater, A.V. 2012. Review of fast pyrolysis of biomass and product upgrading. *Biomass and Bioenergy* 38: 68-94.

Buitrago-Sierra, R., Ruiz-Martínez, J., Serrano-Ruiz, J.C., Rodríguez-Reinoso, F., A. Sepúlveda-Escribano A. 2012. Ethanol Steam Reforming on Ni/Al2O3 Catalysts: Effect of the Addition of Zn and Pt. *Journal of Colloid and Interface Science* 383(1): 148-154.

Dorado, M.P. Ballesteros, E. Arnal,. J. M. Gómez, J. López, F.J. 2003. Exhaust emissions from a diesel engine fueled with transesterified waste olive oil. *Fuel* 82(11): 311-1315.

Gan, P. Y., Li, Z. D. 2008. An econometric study on long-term energy outlook and the implications of renewable energy utilization in Malaysia. *Energy Policy* 36(2):890-899.

Haber, J., Block, J. H., Delmon, B. 1995. Manual of methods and procedures for catalyst characterization. *Pure and Applied Chemistry* 67: 1257-1306.

Hagen, J. 2006. Industrial catalysis: A practical approach. *Wiley-VCH Verlag GmbH & Co.*, 1-14.

Hashim H, Ho, W. S. 2011. Renewable energy policies and initiatives for a sustainable energy future in Malaysia. *Renewable and Sustainable Energy Reviews* 15(9):4780-4787.

Huang, H., Young, N., Williams, B.P. , Taylor, S.H., Hutchings, G. 2005. COS hydrolysis using zinc-promoted alumina catalysts. *Catalysis Letters* 104(1): 17-21.

Kiss, E., Ratkovic, S., Vujicic, D., Boskovic, G. 2012. Accelerated polymorphous transformations of alumina induced by copper ions impede spinal formation. *Indian Journal of Chemistry* 51(A): 1669-1676.

Li, G. 2005. FT-IR studies of zeolite materials: characterization and environmental applications. *The University of Iowa's Institutional Repository*, Ph.D thesis.

McKendry, P. 2002. Energy production from biomass (part 1): overview of biomass. *Bioresource Technology* 83: 37-46

Nascimento, J. C., Sousa, J. F., Rojas, L.O. A., Fontes, F.A.O. 2011. Synthesis and characterization of $CuCl_2$ /SiO_2 catalyst for the oxychlorination of methane. *Brazilian Journal of Petroleum and Gas* 5(2): 55-63.

Ookawa. M. 2012. Synthesis and characterization of Fe-Imogolite as an oxidation catalyst. *InTech*, 239-258.

Pua, F., Fang, Z. Zakaria, S. Z., Guo, F. Chin-Hua, C. 2011. Direct production of biodiesel from high-acid value Jatropha oil with solid acid catalyst derived from lignin. *Biotechnology for Biofuels* 4: 56.

Rosal, R., Gonzalo, M.S., Rodríguez, A., García-Calvo E. 2010. Catalytic ozonation of fenofibric acid over alumina-supported manganese oxide. *Journal of Hazardous Materials* 183(1-3), 271–278.

Zabeti , M., Daud , W.M.A.W., Aroua M.K. 2010. Biodiesel production using alumina-supported calcium oxide: an optimization study. *Fuel Processing Technology* 91(2) 243–248.

Zabeti , M., Daud , W.M.A.W., Aroua M.K. 2009. Optimization of the activity of cao/al2o3 catalyst for biodiesel production using response surface methodology. *Applied Catalysis A: General* 366 (1) 154-159.

COMPLEX INTUITIONISTIC FUZZY SUBRINGS

Mikhled[1*] Okleh Alsarahead, Abd Ghafur[1] Ahmad

[1]School of Mathematical Science,
Faculty of Sciences and Technology,
Universiti Kebangsaan Malaysia, Malaysia.

[*]Corresponding author's email: mekhledsarheed@yahoo.com

ABSTRACT. *In this paper, we defined the complex intuitionistic fuzzy subring and introduced some new concepts like Intuitionistic $\pi-$fuzzy sets and homogeneous complex intuitionistic fuzzy sets. Then, we investigated some of characteristics of complex intuitionistic fuzzy subring. The relationship between complex intuitionistic fuzzy subring and intuitionistic fuzzy subring is also investigated. It is found that every complex intuitionistic fuzzy subring yields two intuitionistic fuzzy subring. Finaly, we defined the image and inverse image of complex intuitionistic fuzzy subring under ring homomorphism, and thus studied their elementary properties.*

KEYWORDS. *Intuitionistic $\pi-$fuzzy set, intuitionistic $\pi-$fuzzy subring, homogeneous complex intuitionistic fuzzy set, complex intuitionistic fuzzy subring.*

INTRODUCTION

After the introduction of the concept of fuzzy set by Zadeh (1965), many researches were conducted on the generalization of the notion of fuzzy set. Atanassov (1986) introduced the concept of intuitionistic fuzzy set. Hur *et al*., (2003) investigated intuitionistic fuzzy subgroups and subrings in 2003. The concept of the complex fuzzy sets was introduced (Ramot *et al.*, 2002). The concept of a complex intuitionistic fuzzy set was introduced by Alkouri *et al.*, (2012). In three recent papers, Alsarahead and Ahmad (2017a; 2017b; 2017c) introduced the concepts of complex fuzzy subgroup, complex fuzzy subring and complex intuitionistic fuzzy subgroup.

In this paper, we defined the complex intuitionistic fuzzy subrings and introduced some new concepts like intuitionistic $\pi-$fuzzy subring. Then, we investigated some of characteristics of complex intuitionistic fuzzy subrings. Finaly, we defined the image and inverse image of complex intuitionistic fuzzy subrings under ring homomorphism, and then we studied their properties.

PRELIMINARIES

Definition 1. Let $A=\{(x,\mu_A(x),\nu_A(x)):x\in R\}$ be an intuitionistic fuzzy set of a ring R. Then, A is said to be an intuitionistic fuzzy subring of R if for all $x,y\in R$ the followings hold:

1. $\mu_A(x-y)\geq min\{\mu_A(x),\mu_A(y)\}$.
2. $\mu_A(xy)\geq min\{\mu_A(x),\mu_A(y)\}$.
3. $\nu_A(x-y)\leq max\{\nu_A(x),\nu_A(y)\}$.
4. $\nu_A(xy)\leq max\{\nu_A(x),\nu_A(y)\}$, Atanassov (1986).

Definition 2. A complex intuitionistic fuzzy set A, defined on a universe of discourse U, is characterized by membership and non-membership functions $\mu_A(x)=r_A(x)e^{i\omega_A(x)}$ and $\nu_A(x)=\hat{r}_A(x)e^{i\hat{\omega}_A(x)}$, respectively, that assign any element $x\in U$ a complex-valued grade of both membership and non-membership in A. By definition,

$A=\{(x,\mu_A(x),\nu_A(x)):x\in U\}$ where $r_A(x)+\hat{r}_A(x)\leq 1$. Alkouri and Salleh (2012).

Definition 3. Let A and B be two complex intuitionistic fuzzy subsets of U, with membership functions $\mu_A(x)=r_A(x)e^{i\omega_A(x)}$ and $\mu_B(x)=r_B(x)e^{i\omega_B(x)}$, respectively, while the non-membership functions are $\nu_A(x)=\hat{r}_A(x)e^{i\hat{\omega}_A(x)}$ and $\nu_B(x)=\hat{r}_B(x)e^{i\hat{\omega}_B(x)}$, respectively. Then $A\cap B$ is given by:

$A\cap B=\{(x,\mu_{A\cap B}(x),\nu_{A\cap B}(x)):x\in U\}$ where

$\mu_{A\cap B}(x)=min\{r_A(x),r_B(x)\}e^{i\,min\{\omega_A(x),\omega_B(x)\}}$

$\nu_{A\cap B}(x)=max\{\hat{r}_A(x),\hat{r}_B(x)\}e^{i\,max\{\hat{\omega}_A(x),\hat{\omega}_B(x)\}}$. Alkouri and Salleh (2012).

Definition 4. Let $A=\{(x,\mu_A(x),\nu_A(x)):x\in U\}$ be a intuitionistic fuzzy set. Then the set $A_\pi=\{(x,\gamma_{A_\pi}(x),\rho_{A_\pi}(x)):x\in U\}$ is said to be intuitionistic $\pi-$fuzzy set where $\gamma_{A_\pi}(x)=2\pi\mu_A(x)$ and $\rho_{A_\pi}(x)=2\pi\nu_A(x)$.

Note that the condition $\gamma_{A_\pi}(x)+\rho_{A_\pi}(x)\leq 2\pi$ is already satisfied. Alsarahead and Ahmad (2017c).

Definition 5. Let $A_\pi=\{(x,\gamma_{A_\pi}(x),\rho_{A_\pi}(x)):x\in U\}$ be an intuitionistic $\pi-$fuzzy set of a ring R. Then A_π is said to be an intuitionistic $\pi-$fuzzy subring of R if for all $x,y\in R$ the following hold:

1. $\gamma_{A_\pi}(x-y) \geq min\{\gamma_{A_\pi}(x), \gamma_{A_\pi}(y)\}$.
2. $\gamma_{A_\pi}(xy) \geq min\{\gamma_{A_\pi}(x), \gamma_{A_\pi}(y)\}$.
3. $\rho_{A_\pi}(x-y) \leq max\{\rho_{A_\pi}(x), \rho_{A_\pi}(y)\}$.
4. $\rho_{A_\pi}(xy) \leq max\{\rho_{A_\pi}(x), \rho_{A_\pi}(y)\}$.

Proposition 6. An intuitionistic $\pi-$fuzzy set A_π is an intuitionistic $\pi-$fuzzy subring if and only if A is an intuitionistic fuzzy subring.
Proof. Clear.

Definition 7. Let A and B be two complex intuitionistic fuzzy subsets of G, with membership functions $\mu_A(x) = r_A(x)e^{i\omega_A(x)}$ and $\mu_B(x) = r_B(x)e^{i\omega_B(x)}$, respectively. While the non-membership functions are $\nu_A(x) = \hat{r}_A(x)e^{i\hat{\omega}_A(x)}$ and $\nu_B(x) = \hat{r}_B(x)e^{i\hat{\omega}_B(x)}$ respectively. Then
1. A complex intuitionistic fuzzy subset A is said to be a homogeneous complex intuitionistic fuzzy set if for all $x, y \in G$ the following hold:

1. $r_A(x) \leq r_A(y)$ if and only if $\omega_A(x) \leq \omega_A(y)$.
2. $\hat{r}_A(x) \leq \hat{r}_A(y)$ if and only if $\hat{\omega}_A(x) \leq \hat{\omega}_A(y)$.

2. A complex intuitionistic fuzzy subset A is said to be homogeneous with B, if for All $x, y \in G$ the following hold:

1. $r_A(x) \leq r_B(y)$ if and only if $\omega_A(x) \leq \omega_B(y)$.
2. $\hat{r}_A(x) \leq \hat{r}_B(y)$ if and only if $\hat{\omega}_A(x) \leq \hat{\omega}_B(y)$. Alsarahead and Ahmad (2017c).

COMPLEX INTUITIONISTIC FUZZY SUBRINGS

Definition 8. Let $A = \{(x, \mu_A(x), \nu_A(x)) : x \in R\}$ be a homogeneous complex intuitionistic fuzzy set of a ring R. Then A is said to be a complex intuitionistic fuzzy subring of R if for all $x, y \in R$ the following hold:

1. $\mu_A(x-y) \geq min\{\mu_A(x), \mu_A(y)\}$.
2. $\mu_A(xy) \geq min\{\mu_A(x), \mu_A(y)\}$.
3. $\nu_A(x-y) \leq max\{\nu_A(x), \nu_A(y)\}$.
4. $\nu_A(xy) \leq max\{\nu_A(x), \nu_A(y)\}$.

Theorem 9. Let R be a ring and $A = \{(x, \mu_A(x), \nu_A(x)) : x \in R\}$ be a homogeneous complex intuitionistic fuzzy set with membership function $\mu_A(x) = r_A(x)e^{i\omega_A(x)}$ and non-membership function $\nu_A(x) = \hat{r}_A(x)e^{i\hat{\omega}_A(x)}$. Then A is a complex intuitionistic fuzzy subring of R if and only if:

1. The intuitionistic fuzzy set $\overline{A} = \{(x, r_A(x), \hat{r}_A(x)) : x \in R, r_A(x), \hat{r}_A(x) \in [0,1]\}$ is an intuitionistic fuzzy subring.
2. The intuitionistic $\pi-$fuzzy set $\underline{A} = \{(x, \omega_A(x), \hat{\omega}_A(x)) : x \in R, \omega_A(x), \hat{\omega}_A(x) \in [0,2\pi]\}$ is an intuitionistic $\pi-$fuzzy subring.

Proof. Let A be a complex intuitionistic fuzzy subring and $x, y \in R$. Then we have

$$\begin{aligned} r_A(x-y)e^{i\omega_A(x-y)} &= \mu_A(x-y) \\ &\geq min\{\mu_A(x), \mu_A(y)\} \\ &= min\left\{r_A(x)e^{i\omega_A(x)}, r_A(y)e^{i\omega_A(y)}\right\} \\ &= min\{r_A(x), r_A(y)\}e^{i\, min\{\omega_A(x), \omega_A(y)\}} \end{aligned}$$

(since A is homogeneous).

So $r_A(x-y) \geq min\{r_A(x), r_A(y)\}$ and $\omega_A(x-y) \geq min\{\omega_A(x), \omega_A(y)\}$. Also, we have

$$\begin{aligned} r_A(xy)e^{i\omega_A(xy)} &= \mu_A(xy) \\ &\geq min\{\mu_A(x), \mu_A(y)\} \\ &= min\left\{r_A(x)e^{i\omega_A(x)}, r_A(y)e^{i\omega_A(y)}\right\} \\ &= min\{r_A(x), r_A(y)\}e^{i\, min\{\omega_A(x), \omega_A(y)\}} \end{aligned}$$

(since A is homogeneous).

which implies $r_A(xy) \geq min\{r_A(x), r_A(y)\}$ and $\omega_A(xy) \geq min\{\omega_A(x), \omega_A(y)\}$. On the other hand

$$\begin{aligned} \hat{r}_A(x-y)e^{i\hat{\omega}_A(x-y)} &= \nu_A(x-y) \\ &\leq max\{\nu_A(x), \nu_A(y)\} \\ &= max\left\{\hat{r}_A(x)e^{i\hat{\omega}_A(x)}, \hat{r}_A(y)e^{i\hat{\omega}_A(y)}\right\} \\ &= max\{\hat{r}_A(x), \hat{r}_A(y)\}e^{i\, max\{\hat{\omega}_A(x), \hat{\omega}_A(y)\}} \end{aligned}$$

(since A is homogeneous).

So $\hat{r}_A(x-y) \leq max\{\hat{r}_A(x), \hat{r}_A(y)\}$ and $\hat{\omega}_A(x-y) \leq max\{\hat{\omega}_A(x), \hat{\omega}_A(y)\}$. Also, we have

$$\begin{aligned} \hat{r}_A(xy)e^{i\hat{\omega}_A(xy)} &= \nu_A(xy) \\ &\leq max\{\nu_A(x), \nu_A(y)\} \\ &= max\left\{\hat{r}_A(x)e^{i\hat{\omega}_A(x)}, \hat{r}_A(y)e^{i\hat{\omega}_A(y)}\right\} \\ &= max\{\hat{r}_A(x), \hat{r}_A(y)\}e^{i\, max\{\hat{\omega}_A(x), \hat{\omega}_A(y)\}} \end{aligned}$$

(since A is homogeneous).

which implies $\hat{r}_A(xy) \le max\{\hat{r}_A(x), \hat{r}_A(y)\}$ and $\hat{\omega}_A(xy) \le max\{\hat{\omega}_A(x), \hat{\omega}_A(y)\}$.
So $\overline{A}$ is an intuitionistic fuzzy subring and $\underline{A}$ is an intuitionistic $\pi-$fuzzy subring.
Conversely, let $\overline{A}$ be an intuitionistic fuzzy subring and $\underline{A}$ be an intuitionistic $\pi-$fuzzy subring.
So we have

$$\begin{aligned} r_A(x-y) &\ge min\{r_A(x), r_A(y)\} & \omega_A(x-y) &\ge min\{\omega_A(x), \omega_A(y)\} \\ r_A(xy) &\ge min\{r_A(x), r_A(y)\} & \omega_A(xy) &\ge min\{\omega_A(x), \omega_A(y)\} \\ \hat{r}_A(x-y) &\le max\{\hat{r}_A(x), \hat{r}_A(y)\} & \hat{\omega}_A(x-y) &\le max\{\hat{\omega}_A(x), \hat{\omega}_A(y)\} \\ \hat{r}_A(xy) &\le max\{\hat{r}_A(x), \hat{r}_A(y)\} & \hat{\omega}_A(xy) &\le max\{\hat{\omega}_A(x), \hat{\omega}_A(y)\}. \end{aligned}$$

Now,

$$\begin{aligned} \mu_A(x-y) = r_A(x-y)e^{i\omega_A(x-y)} &\ge min\{r_A(x), r_A(y)\}e^{i\,min\{\omega_A(x), \omega_A(y)\}} \\ &= min\left\{r_A(x)e^{i\omega_A(x)}, r_A(y)e^{i\omega_A(y)}\right\} \text{ (homogeneity).} \\ &= min\{\mu_A(x), \mu_A(y)\}. \end{aligned}$$

Also, we have

$$\begin{aligned} \mu_A(xy) = r_A(xy)e^{i\omega_A(xy)} &\ge min\{r_A(x), r_A(y)\}e^{i\,min\{\omega_A(x), \omega_A(y)\}} \\ &= min\left\{r_A(x)e^{i\omega_A(x)}, r_A(y)e^{i\omega_A(y)}\right\} \text{ (homogeneity)} \\ &= min\{\mu_A(x), \mu_A(y)\}. \end{aligned}$$

On the other hand

$$\begin{aligned} \nu_A(x-y) = \hat{r}_A(x-y)e^{i\hat{\omega}_A(x-y)} &\le max\{\hat{r}_A(x), \hat{r}_A(y)\}e^{i\,max\{\hat{\omega}_A(x), \hat{\omega}_A(y)\}} \\ &= max\left\{\hat{r}_A(x)e^{i\hat{\omega}_A(x)}, \hat{r}_A(y)e^{i\hat{\omega}_A(y)}\right\} \\ &= max\{\nu_A(x), \nu_A(y)\}. \end{aligned}$$

Also, we have

$$\begin{aligned} \nu_A(xy) = \hat{r}_A(xy)e^{i\hat{\omega}_A(xy)} &\le max\{\hat{r}_A(x), \hat{r}_A(y)\}e^{i\,max\{\hat{\omega}_A(x), \hat{\omega}_A(y)\}} \\ &= max\left\{\hat{r}_A(x)e^{i\hat{\omega}_A(x)}, \hat{r}_A(y)e^{i\hat{\omega}_A(y)}\right\} \\ &= max\{\nu_A(x), \nu_A(y)\}. \end{aligned}$$

So A is a complex intuitionistic fuzzy subring.

Theorem 10. Let $\{A_i : i \in I\}$ be a collection of complex intuitionistic fuzzy subrings of a ring R. Then $\cap_{i\in I} A_i$ is a complex intuitionistic fuzzy subring.

Proof. For all $i \in I$ we have $r_{A_i}(x)$ is an intuitionistic fuzzy subring and $\omega_{A_i}(x)$ is an intuitionistic $\pi-$fuzzy subring (Theorem 9). Now, let $x, y \in G$. Then

$$\mu_{\cap_{i\in I}A_i}(x-y) = r_{\cap_{i\in I}A_i}(x-y)e^{i\omega_{\cap_{i\in I}A_i}(x-y)}$$

$$= min_{i\in I}\left\{r_{A_i}(xy)\right\}e^{i\,min_{i\in I}\left\{\omega_{A_i}(xy)\right\}}$$

$$\geq min_{i\in I}\left\{min\left\{r_{A_i}(x), r_{A_i}(y)\right\}\right\}e^{i\,min_{i\in I}\left\{min\left\{\omega_{A_i}(x),\omega_{A_i}(y)\right\}\right\}}$$

$$= min\left\{min_{i\in I}\left\{r_{A_i}(x)\right\}, min_{i\in I}\left\{r_{A_i}(y)\right\}\right\}e^{i\,min\left\{min_{i\in I}\left\{\omega_{A_i}(x)\right\},min_{i\in I}\left\{\omega_{A_i}(y)\right\}\right\}}$$

$$= min\left\{min_{i\in I}\left\{r_{A_i}(x)\right\}e^{i\,min_{i\in I}\left\{\omega_{A_i}(x)\right\}}, min_{i\in I}\left\{r_{A_i}(y)\right\}e^{i\,min_{i\in I}\left\{\omega_{A_i}(y)\right\}}\right\}$$

$$= min\left\{\mu_{\cap_{i\in I}A_i}(x), \mu_{\cap_{i\in I}A_i}(y)\right\}.$$

Also, we have

$$\mu_{\cap_{i\in I}A_i}(xy) = r_{\cap_{i\in I}A_i}(xy)e^{i\omega_{\cap_{i\in I}A_i}(xy)}$$

$$= min_{i\in I}\left\{r_{A_i}(xy)\right\}e^{i\,min_{i\in I}\left\{\omega_{A_i}(xy)\right\}}$$

$$\geq min_{i\in I}\left\{min\left\{r_{A_i}(x), r_{A_i}(y)\right\}\right\}e^{i\,min_{i\in I}\left\{min\left\{\omega_{A_i}(x),\omega_{A_i}(y)\right\}\right\}}$$

$$= min\left\{min_{i\in I}\left\{r_{A_i}(x)\right\}, min_{i\in I}\left\{r_{A_i}(y)\right\}\right\}e^{i\,min\left\{min_{i\in I}\left\{\omega_{A_i}(x)\right\},min_{i\in I}\left\{\omega_{A_i}(y)\right\}\right\}}$$

$$= min\left\{min_{i\in I}\left\{r_{A_i}(x)\right\}e^{i\,min_{i\in I}\left\{\omega_{A_i}(x)\right\}}, min_{i\in I}\left\{r_{A_i}(y)\right\}e^{i\,min_{i\in I}\left\{\omega_{A_i}(y)\right\}}\right\}$$

$$= min\left\{\mu_{\cap_{i\in I}A_i}(x), \mu_{\cap_{i\in I}A_i}(y)\right\}.$$

On other hand

$$\nu_{\cap_{i\in I}A_i}(x-y) = \hat{r}_{\cap_{i\in I}A_i}(x-y)e^{i\hat{\omega}_{\cap_{i\in I}A_i}(x-y)}$$

$$= max_{i\in I}\left\{\hat{r}_{A_i}(x-y)\right\}e^{i\,max_{i\in I}\left\{\hat{\omega}_{A_i}(x-y)\right\}}$$

$$\leq max_{i\in I}\left\{max\left\{\hat{r}_{A_i}(x), r_{A_i}(y)\right\}\right\}e^{i\,max_{i\in I}\left\{max\left\{\hat{\omega}_{A_i}(x),\hat{\omega}_{A_i}(y)\right\}\right\}}$$

$$= max\left\{ max_{i\in I}\left\{\hat{r}_{A_i}(x)\right\}, max_{i\in I}\left\{\hat{r}_{A_i}(y)\right\}\right\} e^{i max\left\{ max_{i\in I}\left\{\hat{\omega}_{A_i}(x)\right\}, max_{i\in I}\left\{\hat{\omega}_{A_i}(y)\right\}\right\}}$$

$$= max\left\{ max_{i\in I}\left\{\hat{r}_{A_i}(x)\right\} e^{i max_{i\in I}\left\{\hat{\omega}_{A_i}(x)\right\}},\ max_{i\in I}\left\{\hat{r}_{A_i}(y)\right\} e^{i max_{i\in I}\left\{\hat{\omega}_{A_i}(y)\right\}} \right\}$$

$$= max\left\{ \nu_{\cap_{i\in I} A_i}(x), \nu_{\cap_{i\in I} A_i}(y)\right\}.$$

Also, we have

$$\nu_{\cap_{i\in I} A_i}(xy) = \hat{r}_{\cap_{i\in I} A_i}(xy) e^{i\hat{\omega}_{\cap_{i\in I} A_i}(xy)}$$

$$= max_{i\in I}\left\{\hat{r}_{A_i}(xy)\right\} e^{i max_{i\in I}\left\{\hat{\omega}_{A_i}(xy)\right\}}$$

$$\le max_{i\in I}\left\{max\left\{\hat{r}_{A_i}(x), \hat{r}_{A_i}(y)\right\}\right\} e^{i max_{i\in I}\left\{max\left\{\hat{\omega}_{A_i}(x), \hat{\omega}_{A_i}(y)\right\}\right\}}$$

$$= max\left\{ max_{i\in I}\left\{\hat{r}_{A_i}(x)\right\}, max_{i\in I}\left\{\hat{r}_{A_i}(y)\right\}\right\} e^{i max\left\{ max_{i\in I}\left\{\hat{\omega}_{A_i}(x)\right\}, max_{i\in I}\left\{\hat{\omega}_{A_i}(y)\right\}\right\}}$$

$$= max\left\{ max_{i\in I}\left\{\hat{r}_{A_i}(x)\right\} e^{i max_{i\in I}\left\{\hat{\omega}_{A_i}(x)\right\}},\ max_{i\in I}\left\{\hat{r}_{A_i}(y)\right\} e^{i max_{i\in I}\left\{\hat{\omega}_{A_i}(y)\right\}} \right\}$$

$$= max\left\{ \nu_{\cap_{i\in I} A_i}(x), \nu_{\cap_{i\in I} A_i}(y)\right\}.$$

Definition 11. Let $A = \left\{\left(x, \mu_A(x), \nu_A(x)\right) : x \in U\right\}$ be a complex intuitionistic fuzzy set with membership function $\mu_A(x) = r_A(x)e^{i\omega_A(x)}$ and non-membership function $\nu_A(x) = \hat{r}_A(x)e^{i\hat{\omega}_A(x)}$. For $\alpha, \hat{\alpha} \in [0,1]$ and $\beta, \hat{\beta} \in [0, 2\pi]$, the set $A^{(\hat{\alpha},\hat{\beta})}_{(\alpha,\beta)} = \{x \in U : r_A(x) \ge \alpha, \omega_A(x) \ge \beta, \hat{r}_A(x) \le \hat{\alpha}, \hat{\omega}_A(x) \le \hat{\beta}\}$ is called a level subset of the complex intuitionistic fuzzy subset A. In particular if $\beta = \hat{\beta} = 0$, then we get the level subset $A^{\hat{\alpha}}_{\alpha} = \{x \in U : r_A(x) \ge \alpha, \hat{r}_A(x) \le \hat{\alpha}\}$. If $\alpha = \hat{\alpha} = 0$, then we get the level subset $A^{\hat{\beta}}_{\beta} = \{x \in U : \omega_A(x) \ge \beta, \hat{\omega}_A(x) \le \hat{\beta}\}$. Alsarahead and Ahmad (2017c).

Theorem 12. Let $A = \left\{\left(x, \mu_A(x), \nu_A(x)\right) : x \in R\right\}$ be a complex intuitionistic fuzzy subring of R with membership function $\mu_A(x) = r_A(x)e^{i\omega_A(x)}$ and non-membership function $\nu_A(x) = \hat{r}_A(x)e^{i\hat{\omega}_A(x)}$, if $r_A(e) \ge \alpha$, $\omega_A(e) \ge \beta$, $\hat{r}_A(e) \le \hat{\alpha}$ and $\hat{\omega}_A(e) \le \hat{\beta}$. Then the level subset $A^{(\hat{\alpha},\hat{\beta})}_{(\alpha,\beta)}$ is a subring of R.

Proof. $e \in A^{(\hat{\alpha},\hat{\beta})}_{(\alpha,\beta)}$, so $A^{(\hat{\alpha},\hat{\beta})}_{(\alpha,\beta)} \neq \phi$. Let $x, y \in A^{(\hat{\alpha},\hat{\beta})}_{(\alpha,\beta)}$. Then we have $r_A(x) \geq \alpha$, $\omega_A(x) \geq \beta$, $\hat{r}_A(x) \leq \hat{\alpha}$ and $\hat{\omega}_A(x) \leq \hat{\beta}$, also, $r_A(y) \geq \alpha$, $\omega_A(y) \geq \beta$, $\hat{r}_A(y) \leq \hat{\alpha}$ and $\hat{\omega}_A(y) \leq \hat{\beta}$.

Now,

$$\begin{aligned} r_A(x-y)e^{i\omega_A(x-y)} = \mu_A(x-y) &\geq min\{\mu_A(x), \mu_A(y)\} \\ &= min\left\{r_A(x)e^{i\omega_A(x)}, r_A(y)e^{i\omega_A(y)}\right\} \\ &= min\{r_A(x), r_A(y)\}e^{i\,min\{\omega_A(x),\omega_A(y)\}} \end{aligned}$$

This implies

$$\begin{aligned} r_A(x-y) &\geq min\{r_A(x), r_A(y)\} \\ &\geq min\{\alpha, \alpha\} \\ &= \alpha. \end{aligned}$$

And

$$\begin{aligned} \omega_A(x-y) &\geq min\{\omega_A(x), \omega_A(y)\} \\ &\geq min\{\beta, \beta\} \\ &= \beta. \end{aligned}$$

Also, we have

$$\begin{aligned} \hat{r}_A(x-y)e^{i\hat{\omega}_A(x-y)} = \nu_A(x-y) &\leq max\{\nu_A(x), \nu_A(y)\} \\ &= max\left\{\hat{r}_A(x)e^{i\hat{\omega}_A(x)}, \hat{r}_A(y)e^{i\hat{\omega}_A(y)}\right\} \\ &= max\{\hat{r}_A(x), \hat{r}_A(y)\}e^{i\,max\{\hat{\omega}_A(x),\hat{\omega}_A(y)\}} \end{aligned}$$

This implies

$$\begin{aligned} \hat{r}_A(x-y) &\leq max\{\hat{r}_A(x), \hat{r}_A(y)\} \\ &\leq max\{\hat{\alpha}, \hat{\alpha}\} \\ &= \hat{\alpha}. \end{aligned}$$

And

$$\begin{aligned} \hat{\omega}_A(x-y) &\leq max\{\hat{\omega}_A(x), \hat{\omega}_A(y)\} \\ &\leq max\{\hat{\beta}, \hat{\beta}\} \\ &= \hat{\beta}. \end{aligned}$$

So $x - y \in A^{(\hat{\alpha},\hat{\beta})}_{(\alpha,\beta)}$. On the other hand

$$\begin{aligned} r_A(xy)e^{i\omega_A(xy)} = \mu_A(xy) &\geq min\{\mu_A(x), \mu_A(y)\} \\ &= min\left\{r_A(x)e^{i\omega_A(x)}, r_A(y)e^{i\omega_A(y)}\right\} \\ &= min\{r_A(x), r_A(y)\}e^{i\,min\{\omega_A(x),\omega_A(y)\}} \end{aligned}$$

This implies

$$\begin{aligned} r_A(xy) &\geq min\{r_A(x), r_A(y)\} \\ &\geq min\{\alpha, \alpha\} \\ &= \alpha. \end{aligned}$$

And

$$\begin{aligned} \omega_A(xy) &\geq min\{\omega_A(x), \omega_A(y)\} \\ &\geq min\{\beta, \beta\} \\ &= \beta. \end{aligned}$$

Also, we have

$$\begin{aligned} \hat{r}_A(xy)e^{i\hat{\omega}_A(xy)} &= \nu_A(xy) \leq max\{\nu_A(x), \nu_A(y)\} \\ &= max\left\{\hat{r}_A(x)e^{i\hat{\omega}_A(x)}, \hat{r}_A(y)e^{i\hat{\omega}_A(y)}\right\} \\ &= max\{\hat{r}_A(x), \hat{r}_A(y)\}e^{i\,max\{\hat{\omega}_A(x), \hat{\omega}_A(y)\}} \end{aligned}$$

This implies

$$\begin{aligned} \hat{r}_A(xy) &\leq max\{\hat{r}_A(x), \hat{r}_A(y)\} \\ &\leq max\{\hat{\alpha}, \hat{\alpha}\} \\ &= \hat{\alpha}. \end{aligned}$$

And

$$\begin{aligned} \hat{\omega}_A(xy) &\leq max\{\hat{\omega}_A(x), \hat{\omega}_A(y)\} \\ &\leq max\{\hat{\beta}, \hat{\beta}\} \\ &= \hat{\beta}. \end{aligned}$$

Thus $xy \in A^{(\hat{\alpha},\hat{\beta})}_{(\alpha,\beta)}$, therefore $A^{(\hat{\alpha},\hat{\beta})}_{(\alpha,\beta)}$ is a subring of R.

HOMOMORPHISM

Theorem 13. Let $f: R \to S$ be a ring epimorphism. Let A be an intuitionistic fuzzy subring of R and B be an intuitionistic fuzzy subring of S. Then the inverse image of B is an intuitionistic fuzzy subring of R and the image of A is an intuitionistic fuzzy subring of S. Banerjee and Basnet (2003).
We are going to generalize this result to the complex intuitionistic fuzzy subrings.

Definition 14. Let $f: R \to S$ be a homomorphism. Let $A = \{(x, \mu_A(x), \nu_A(x)) : x \in R\}$ and $B = \{(x, \mu_B(x), \nu_B(x)) : x \in S\}$ be complex intuitionistic fuzzy subrings.

Then $C = \{(y, f(\mu_A)(y), f(\nu_A)(y)) : y \in S\}$ is called image of A, where

$$f(\mu_A)(y) = \begin{cases} \vee\{\mu_A(x) : x \in R, f(x) = y\} & \text{if } f^{-1}(y) \neq \phi \\ 0, & \text{otherwise} \end{cases}$$

$$f(\nu_A)(y) = \begin{cases} \wedge\{\nu_A(x) : x \in R, f(x) = y\} & \text{if } f^{-1}(y) \neq \phi \\ 1, & \text{otherwise} \end{cases}$$

for all $y \in S$.

The set $D = \{(x, f^{-1}(\mu_B)(x), f^{-1}(\nu_B)(x)) : x \in R\}$ is called inverse image of B, where $f^{-1}(\mu_B)(x) = \mu_B(f(x))$ and $f^{-1}(\nu_B)(x) = \nu_B(f(x))$ for all $x \in R$.

Lemma 15. Let $f : R \to S$ be a ring homomorphism. Let A be a complex intuitionistic fuzzy subring of R and B be a complex intuitionistic fuzzy subring of S, with membership functions $\mu_A(x) = r_A(x)e^{i\omega_A(x)}$ and $\mu_B(x) = r_B(x)e^{i\omega_B(x)}$, respectively, while the non-membership functions are $\nu_A(x) = \hat{r}_A(x)e^{i\hat{\omega}_A(x)}$ and $\nu_B(x) = \hat{r}_B(x)e^{i\hat{\omega}_B(x)}$, respectively. Then

1. $f(\mu_A)(y) = f(r_A)(y)e^{if(\omega_A)(y)}$.
2. $f(\nu_A)(y) = f(\hat{r}_A)(y)e^{if(\hat{\omega}_A)(y)}$.
3. $f^{-1}(\mu_B)(x) = f^{-1}(r_B)(x)e^{if^{-1}(\omega_B)(x)}$.
4. $f^{-1}(\nu_B)(x) = f^{-1}(\hat{r}_B)(x)e^{if^{-1}(\hat{\omega}_B)(x)}$.

Proof.(1)

$$\begin{aligned} f(\mu_A)(y) &= max_{f(x)=y}\mu_A(x) \\ &= max_{f(x)=y}r_A(x)e^{i\omega_A(x)} \\ &= max_{f(x)=y}r_A(x)e^{i\,max_{f(x)=y}\omega_A(x)} \\ &\text{(since } A \text{ is homogeneous)} \\ &= f(r_A)(y)e^{if(\omega_A)(y)}. \end{aligned}$$

2)

$$\begin{aligned} f(\nu_A)(y) &= min_{f(x)=y}\nu_A(x) \\ &= min_{f(x)=y}\hat{r}_A(x)e^{i\hat{\omega}_A(x)} \\ &= min_{f(x)=y}\hat{r}_A(x)e^{i\,min_{f(x)=y}\hat{\omega}_A(x)} \\ &\text{(since } A \text{ is homogeneous)} \\ &= f(\hat{r}_A)(y)e^{if(\hat{\omega}_A)(y)}. \end{aligned}$$

(3)

$$f^{-1}(\mu_B)(x) = \mu_B\big(f(x)\big)$$
$$= r_B(f(x))e^{i\omega_B(f(x))}$$
$$= f^{-1}(r_B)(x)e^{if^{-1}(\omega_B)(x)}.$$

(4)

$$f^{-1}(\nu_B)(x) = \nu_B\big(f(x)\big)$$
$$= \hat{r}_B(f(x))e^{i\hat{\omega}_B(f(x))}$$
$$= f^{-1}(\hat{r}_B)(x)e^{if^{-1}(\hat{\omega}_B)(x)}.$$

Theorem 16. Let $f: R \to S$ be a ring epimorphism. Let A be a complex intuitionistic fuzzy subring of R with membership function $\mu_A(x) = r_A(x)e^{i\omega_A(x)}$ and non-membership function $\nu_A(x) = \hat{r}_A(x)e^{i\hat{\omega}_A(x)}$. Then the image of A is a complex intuitionistic fuzzy subring of S.

Proof. Since A is a complex intuitionistic fuzzy subring, then by (Theorem 9) $\{(x, r_A(x), \hat{r}_A(x)) : x \in R\}$ is an intuitionistic fuzzy subring and $\{(x, \omega_A(x), \hat{\omega}_A(x)) : x \in R\}$ is an intuitionistic $\pi-$fuzzy subring. Thus by (Theorem 13) and (Proposition 6) the image of $\{(x, r_A(x), \hat{r}_A(x)) : x \in R\}$ and $\{(x, \omega_A(x), \hat{\omega}_A(x)) : x \in R\}$ are intuitionistic fuzzy subring and intuitionistic $\pi-$fuzzy subring, respectively, therefore for all $x, y \in S$ we have:

$$f(r_A)(x-y) \geq \min\{f(r_A)(x), f(r_A)(y)\},\ f(r_A)(xy) \geq \min\{f(r_A)(x), f(r_A)(y)\}$$
$$f(\hat{r}_A)(x-y) \leq \max\{f(\hat{r}_A)(x), f(\hat{r}_A)(y)\},\ f(\hat{r}_A)(xy) \leq \max\{f(\hat{r}_A)(x), f(\hat{r}_A)(y)\}$$
$$f(\omega_A)(x-y) \geq \min\{f(\omega_A)(x), f(\omega_A)(y)\}, f(\omega_A)(xy) \geq \min\{f(\omega_A)(x), f(\omega_A)(y)\}$$
$$f(\hat{\omega}_A)(x-y) \leq \max\{f(\hat{\omega}_A)(x), f(\hat{\omega}_A)(y)\} \text{ and } f(\hat{\omega}_A)(xy) \leq \max\{f(\hat{\omega}_A)(x), f(\hat{\omega}_A)(y)\}$$

Now, by Lemma 15

$$f(\mu_A)(x-y) = f(r_A)(x-y)e^{if(\omega_A)(x-y)}$$
$$\geq min\{f(r_A)(x), f(r_A)(y)\}e^{imin\{f(\omega_A)(x), f(\omega_A)(y)\}}$$
$$= min\{f(r_A)(x)e^{if(\omega_A)(x)}, f(r_A)(y)e^{if(\omega_A)(y)}\}$$
$$= min\{f(\mu_A)(x), f(\mu_A)(y)\}.$$

Also,

$$f(\mu_A)(xy) = f(r_A)(xy)e^{if(\omega_A)(xy)}$$
$$\geq min\{f(r_A)(x), f(r_A)(y)\}e^{imin\{f(\omega_A)(x), f(\omega_A)(y)\}}$$
$$= min\{f(r_A)(x)e^{if(\omega_A)(x)}, f(r_A)(y)e^{if(\omega_A)(y)}\}$$

$$= min\{f(\mu_A)(x), f(\mu_A)(y)\}.$$

On the other hand

$$\begin{aligned} f(\nu_A)(x-y) &= f(\hat{r}_A)(x-y)e^{if(\hat{\omega}_A)(x-y)} \\ &\le max\{f(\hat{r}_A)(x), f(\hat{r}_A)(y)\}e^{imax\{f(\hat{\omega}_A)(x), f(\hat{\omega}_A)(y)\}} \\ &= max\left\{f(\hat{r}_A)(x)e^{if(\hat{\omega}_A)(x)}, f(\hat{r}_A)(y)e^{if(\hat{\omega}_A)(y)}\right\} \\ &= max\{f(\nu_A)(x), f(\nu_A)(y)\}. \end{aligned}$$

Also,

$$\begin{aligned} f(\nu_A)(xy) &= f(\hat{r}_A)(xy)e^{if(\hat{\omega}_A)(xy)} \\ &\le max\{f(\hat{r}_A)(x), f(\hat{r}_A)(y)\}e^{imax\{f(\hat{\omega}_A)(x), f(\hat{\omega}_A)(y)\}} \\ &= max\left\{f(\hat{r}_A)(x)e^{if(\hat{\omega}_A)(x)}, f(\hat{r}_A)(y)e^{if(\hat{\omega}_A)(y)}\right\} \\ &= max\{f(\nu_A)(x), f(\nu_A)(y)\}. \end{aligned}$$

Theorem 17. Let $f: R \to S$ be a ring epimorphism. Let B be a complex intuitionistic fuzzy subring of S, with membership function $\mu_B(x) = r_B(x)e^{i\omega_B(x)}$ and non-membership function $\nu_B(x) = \hat{r}_B(x)e^{i\hat{\omega}_B(x)}$. Then the inverse image of B is a complex intuitionistic fuzzy subring of R.

Proof. Since B is a complex intuitionistic fuzzy subring, then by (Theorem 9) $\{(x, r_B(x), \hat{r}_B(x)) : x \in S\}$ is an intuitionistic fuzzy subring and $\{(x, \omega_B(x), \hat{\omega}_B(x)) : x \in S\}$ is an intuitionistic $\pi-$fuzzy subring. Thus by (Theorem 15) and (Proposition 6) the inverse image of $\{(x, r_B(x), \hat{r}_B(x)) : x \in S\}$ and $\{(x, \omega_B(x), \hat{\omega}_B(x)) : x \in S\}$ are intuitionistic fuzzy subring and intuitionistic $\pi-$fuzzy subring, respectively, therefore for all $x, y \in R$ we have:

$f^{-1}(r_B)(x-y) \ge \min\left\{f^{-1}(r_B)(x), f^{-1}(r_B)(y)\right\},$
$f^{-1}(r_B)(xy) \ge \min\left\{f^{-1}(r_B)(x), f^{-1}(r_B)(y)\right\},$
$f^{-1}(\hat{r}_B)(x-y) \le \max\left\{f^{-1}(\hat{r}_B)(x), f^{-1}(\hat{r}_B)(y)\right\},$
$f^{-1}(\hat{r}_B)(xy) \le \max\left\{f^{-1}(\hat{r}_B)(x), f^{-1}(\hat{r}_B)(y)\right\},$
$f^{-1}(\omega_B)(x-y) \ge \min\left\{f^{-1}(\omega_B)(x), f^{-1}(\omega_B)(y)\right\},$
$f^{-1}(\omega_B)(xy) \ge \min\left\{f^{-1}(\omega_B)(x), f^{-1}(\omega_B)(y)\right\},$
$f^{-1}(\hat{\omega}_B)(x-y) \le \max\left\{f^{-1}(\hat{\omega}_B)(x), f^{-1}(\hat{\omega}_B)(y)\right\}$ and
$f^{-1}(\hat{\omega}_B)(xy) \le \max\left\{f^{-1}(\hat{\omega}_B)(x), f^{-1}(\hat{\omega}_B)(y)\right\}$

Now, by Lemma 15

$$\begin{aligned} f^{-1}(\mu_B)(x-y) &= f^{-1}(r_B)(x-y)e^{if^{-1}(\omega_B)(x-y)} \\ &\geq min\left\{f^{-1}(r_B)(x), f^{-1}(r_B)(y)\right\}e^{imin\left\{f^{-1}(\omega_B)(x), f^{-1}(\omega_B)(y)\right\}} \\ &= min\left\{f^{-1}(r_B)(x)e^{if^{-1}(\omega_B)(x)}, f^{-1}(r_B)(y)e^{if^{-1}(\omega_B)(y)}\right\} \\ &= min\left\{f^{-1}(\mu_B)(x), f^{-1}(\mu_B)(y)\right\}. \end{aligned}$$

Also,

$$\begin{aligned} f^{-1}(\mu_B)(xy) &= f^{-1}(r_B)(xy)e^{if^{-1}(\omega_B)(xy)} \\ &\geq min\left\{f^{-1}(r_B)(x), f^{-1}(r_B)(y)\right\}e^{imin\left\{f^{-1}(\omega_B)(x), f^{-1}(\omega_B)(y)\right\}} \\ &= min\left\{f^{-1}(r_B)(x)e^{if^{-1}(\omega_B)(x)}, f^{-1}(r_B)(y)e^{if^{-1}(\omega_B)(y)}\right\} \\ &= min\left\{f^{-1}(\mu_B)(x), f^{-1}(\mu_B)(y)\right\}. \end{aligned}$$

On the other hand

$$\begin{aligned} f^{-1}(\nu_B)(x-y) &= f^{-1}(\hat{r}_B)(x-y)e^{if^{-1}(\hat{\omega}_B)(x-y)} \\ &\leq max\left\{f^{-1}(\hat{r}_B)(x), f^{-1}(\hat{r}_B)(y)\right\}e^{imax\left\{f^{-1}(\hat{\omega}_B)(x), f^{-1}(\hat{\omega}_B)(y)\right\}} \\ &= max\left\{f^{-1}(\hat{r}_B)(x)e^{if^{-1}(\hat{\omega}_B)(x)}, f^{-1}(\hat{r}_B)(y)e^{if^{-1}(\hat{\omega}_B)(y)}\right\} \\ &= max\left\{f^{-1}(\nu_B)(x), f^{-1}(\nu_B)(y)\right\}. \end{aligned}$$

Also,

$$\begin{aligned} f^{-1}(\nu_B)(xy) &= f^{-1}(\hat{r}_B)(xy)e^{if^{-1}(\hat{\omega}_B)(xy)} \\ &\leq max\left\{f^{-1}(\hat{r}_B)(x), f^{-1}(\hat{r}_B)(y)\right\}e^{imax\left\{f^{-1}(\hat{\omega}_B)(x), f^{-1}(\hat{\omega}_B)(y)\right\}} \\ &= max\left\{f^{-1}(\hat{r}_B)(x)e^{if^{-1}(\hat{\omega}_B)(x)}, f^{-1}(\hat{r}_B)(y)e^{if^{-1}(\hat{\omega}_B)(y)}\right\} \\ &= max\left\{f^{-1}(\nu_B)(x), f^{-1}(\nu_B)(y)\right\}. \end{aligned}$$

REFERENCES

Alkouri, A. & Salleh A. 2012. *Complex intuitionistic fuzzy sets*, in Proceedings of the International Conference on Fundamental and Applied Sciences (ICFAS '12), vol. 1482 of AIP Confere Proceedings, (2012) 464-470.

Alsarahead, M. & Ahmad, A. 2017a. *Complex Fuzzy Subgroups*, Applied Mathematical Sciences, 11 (41):2011-2021.

Alsarahead, M. & Ahmad, A. 2017b. *Complex Fuzzy Subrings*, International Journal of Pure and Applied Mathematics, accepted for publication.

Alsarahead, M. & Ahmad, A. 2017c. *Complex Intuitionistic Fuzzy Subgroups*, submitted to Italian Journal of Pure and Applied Mathematics.

Atanassov, K.T. 1986. *Intuitionistic fuzzy sets*, Fuzzy Sets and Systems, 20 (1): 87-96.

Hur, K. Kang, H.W. & Song, H.K. 2003. *Intuitionistic fuzzy subgroups and subrings*, Honam Mathematical Journal, 25 (2): 19-41.

Ramot, D. Milo, R. Friedman, M. & Kandel, A. 2002. *Complex fuzzy sets*, IEEE Transaction on Fuzzy Systems, 10 (2):171-186.

Banerjee, B. & Basnet, D.K. 2003. *Intuitionistic fuzzy subrings and ideals*, The Journal of Fuzzy Mathematics, **11** :139-155.

Zadeh, L.A. 1965. *Fuzzy sets*, Information and Control, **8** :338-353.

ON THE GENERAL SOLUTION OF 2TH ORDER LINEAR DIFFERENTIAL EQUATION

J. López-Bonilla, G. Posadas-Durán, O. Salas-Torres

ESIME-Zacatenco, Instituto Politécnico Nacional,
Edif. 4, 1er. Piso, Col. Lindavista CP 07738, CDMX, México.
Email: lopezb@ipn.mx

ABSTRACT. *We employ a method of factorization to obtain the general solution of the second order linear differential equation, which is an alternative procedure to the usual Variation of Parameters method of Lagrange. We consider that our approach can be adapted to linear differential equations of the third and fourth order.*

KEYWORDS. Linear differential equation of second order, Variation of parameters, Factorization method.

INTRODUCTION

We consider the linear differential equation:

$$p(x)y'' + q(x)y' + r(x)y = \phi(x), \tag{1}$$

if the solution $y_1(x)$ of the corresponding homogeneous equation is known, then:

$$py_1'' + qy_1' + ry_1 = 0. \tag{2}$$

In Sec. 2 we show that the factorization:

$$y(x) = y_1(x)\, v(x), \tag{3}$$

, allows to determine the general solution of (1), in harmony with the method of variation of parameters of Lagrange [1-3]. Our procedure is an alternative to several approaches to solve (1) [4-10], and we consider that it can be applied to differential equations of the third and fourth order [11, 12].

GENERAL SOLUTION VIA FACTORIZATION

If we employ (2) and (3) into (1) we obtain the expression:

$$p\, y_1\, v'' + (2p\, y_1' + q\, y_1)\, v' = \phi, \tag{4}$$

where we can introduce the function $u(x) = v'$ to deduce the equation:

$$u' + \left(\frac{q}{p} + \frac{2y_1'}{y_1}\right) u = \frac{\phi}{p\, y_1}\,, \tag{5}$$

that is:

$$\frac{d}{dx}\left(\frac{y_1^2}{W}\, u\right) = \frac{y_1\, \phi}{p\, W}\,, \qquad W = \exp\left(-\int^x \frac{q}{p}\, d\xi\right), \tag{6}$$

whose solution is immediate:

$$u = \frac{dv}{dx} = \frac{W}{y_1^2} \int^x \frac{y_1\, \phi}{p\, W}\, d\eta + c_2\, \frac{W}{y_1^2}\,. \tag{7}$$

Therefore, (3) and the integration of (7) imply the general solution of (1):

$$y(x) = c_1 y_1(x) + c_2 y_2(x) + y_p(x), \tag{8}$$

where:

$$y_2(x) = y_1(x) \int^x \frac{W}{y_1^2}\, d\eta\,, \tag{9}$$

$$y_p(x) = y_1(x) \int^x \frac{W(\varphi)}{y_1^2(\varphi)}\, d\varphi \int^\varphi \frac{y_1(\eta)\, \phi(\eta)}{p(\eta)\, W(\eta)}\, d\eta\,. \tag{10}$$

In (10) we can apply the method of integration by parts, thus giving:

$$y_p(x) \overset{(9)}{=} y_1(x) \left[\frac{y_2(x)}{y_1(x)} \int^x \frac{y_1\, \phi}{p\, W} d\eta - \int^x \frac{y_2\, \phi}{p\, W} d\eta\right] = y_2(x) \int^x \frac{y_1\, \phi}{p\, W}\, d\eta - y_1(x) \int^x \frac{y_2\, \phi}{p\, W}\, d\eta\,, \tag{11}$$

which is in agreement with the method of variation of parameters of Lagrange [1-3].

Our approach shows that the factorization (3) and one solution of (2) allow deduce the general solution of (1), without the *ansatz* of Lagrange in his procedure of variation of parameters.

REFERENCES

A. Hernández-Galeana, J. López-Bonilla, R. López-Vázquez, *On the second order linear differential equation*, Pure and Appl. Maths. Lett. **2** (2014) 31-34.

G. Bahadur Thapa, A. Domínguez-Pacheco, J. López-Bonilla, *On the linear differential equation of second order*, Prespacetime Journal **6**, No. 10 (2015) 999-1001.

*G. Krishna Srinivasan, A note on Lagrange's method of variation of parameters, Missouri J. Math. Sci.**19** (2007) 11-14.*

J. H. Caltenco, J. López-Bonilla, J. Morales, G. Ovando, *On an iterative method to solve 2th order homogeneous linear differential equations*, Inform. Sci. Comput. No. 1 (2014) 1-8.

A. Hernández-Galeana, J. López-Bonilla, R. López-Vázquez, *On the second order linear differential equation*, Pure and Appl. Maths. Lett. **2** (2014) 31-34.

J. López-Bonilla, A. Zaldívar-Sandoval, J. Yaljá Montiel, *2th order linear differential operator in its exact form*, J. Vect. Rel. **5**, No. 1 (2010) 139-141.

J. López-Bonilla, S. Vidal-Beltrán, S. Yáñez-San Agustín, *Homogeneous linear differential equation of second order*, Prespacetime Journal **7**, No. 13 (2016) 1786-1788.

J. López-Bonilla, G. Posadas-Durán, O. Salas-Torres, *Variational principle for* $py'' + qy' + ry = \phi$, Prespacetime Journal **8**, No. 2 (2017) 226-228.

J. López-Bonilla, B. Man Tuladhar, B. Moreno-Ley, *On the 3rd. order linear differential equation*, Kathmandu Univ. J. Sci. Eng. & Techn. **8**, No. 2 (2012) 7-10.

T. Quinn, S. Rai, *Variation of parameters in differential equations*, PRIMUS **23**, No. 1 (2012) 25-44.

V. Barrera F., J. López-Bonilla, R. López-Vázquez, *On the particular solution of* $py'' + qy' + ry = \phi$, Prespacetime Journal **7**, No. 12 (2016) 1677-1679.

Z. Ahsan, *Differential equations and their applications*, Prentice-Hall, New Delhi (2004).

Z. Ahsan, R. Cruz-Santiago, J. López-Bonilla, *Linear differential equations of third and fourth order*, Aligarh Bull. Maths. **31**, No. 1 (2012) 5-7

ON THE ROOTS OF THE LEGENDRE, LAGUERRE, AND HERMITE POLYNOMIALS

S. Álvarez-Ballesteros, J. López-Bonilla, R. López-Vázquez,

ESIME-Zacatenco, Instituto Politécnico Nacional,
Edif. 5, 1er. Piso, Col. Lindavista CP 07738, CDMX, México
*jlopezb@ipn.mx

ABSTRACT. *For several orthogonal polynomials, Cohen proved that their roots are the eigenvalues of symmetric tridiagonal matrices. In this paper, we give examples of this Cohen's result for the Legendre, Laguerre, and Hermite polynomials, which are useful in applications to quantum mechanics and numerical analysis.*

KEYWORDS: Laguerre and Hermite polynomials, Leverrier-Takeno's technique, Legendre polynomials.

INTRODUCTION

Here we consider the Legendre polynomials $P_n(x)$ [1, 2]:

$$P_0(x) = 1, \qquad P_1(x) = x, \qquad P_2(x) = \tfrac{1}{2}(3x^2 - 1), \qquad P_3(x) = \tfrac{1}{2}(5x^3 - 3x), \ldots \tag{1}$$

which verify the differential equation $(1 - x^2)y'' - 2xy' + l(l+1) = 0, \;\; l = 0, 1, 2, \ldots$; Cohen [3, 4] showed that roots of $P_n(x) = 0$ are the proper values of the following symmetric tridiagonal matrix:

$$\boldsymbol{P}_n = \begin{pmatrix} 0 & \frac{1}{\sqrt{3}} & \square & \square & \square & \square & \\ \frac{1}{\sqrt{3}} & 0 & \frac{2}{\sqrt{15}} & \square & \square & \square & \square \\ \square & \frac{2}{\sqrt{15}} & 0 & \frac{3}{\sqrt{35}} & \square & \square & \square \\ \square & \square & \frac{3}{\sqrt{35}} & 0 & \ddots & \square & \square \\ \square & \square & \square & \ddots & \ddots & \ddots & \square \\ \square & \square & \square & \square & \ddots & 0 & g(n) \\ \square & \square & \square & \square & \square & g(n) & 0 \end{pmatrix}, \qquad g(n) = \frac{n-1}{\sqrt{(2n-1)(2n-3)}}. \tag{2}$$

Since the eigenvalues of a symmetric matrix are all real, it follows that the roots of the Legendre polynomials must all be real [1, 5, 6]. Moreover, the absence of nonzero terms along the leading diagonal of the matrix $\boldsymbol{P}_n$ implies that the eigenvalues are symmetrically

distributed about the origin. Let's remember that the roots of $P_n(x)$ are important in the Gaussian quadrature [1, 7].

Similarly, the roots of the Laguerre polynomials $L_n(x)$ [8-10] as:

$$L_0(x)=1,\quad L_1(x)=1-x,\quad L_2(x)=\tfrac{1}{2}(x^2-4x+2),\quad L_3(x)=\tfrac{1}{6}(-x^3+9x^2-18x+6)\ ,\ldots \tag{3}$$

which satisfy the differential equation $xy''+(1-x)y'+ny=0,\ n=0,1,2,\ldots$, are the eigenvalues of the symmetric matrix [3, 4]:

$$\boldsymbol{L}_n=\begin{pmatrix} 1 & 1 & & & & & \\ 1 & 3 & 2 & & & & \\ & 2 & 5 & \ddots & & & \\ & & \ddots & \ddots & \ddots & & \\ & & & \ddots & n-2 & 2n-3 & n-1 \\ & & & & & n-1 & 2n-1 \end{pmatrix}, \tag{4}$$

Hence, all solutions of $L_n(x)=0$ are real [11].

Besides, the Hermite polynomials $H_n(x)$ [12, 13] which are:

$$H_0(x)=1,\qquad H_1(x)=2x,\qquad H_2(x)=4x^2-2,\qquad H_3(x)=8x^3-12x,\ldots \tag{5}$$

obey the differential equation $y''-2xy'+2ny=0,\ n=0,1,2,\ldots$, have real roots [14-16] corresponding to the proper values of [17]:

$$\boldsymbol{H}_n=\begin{pmatrix} 0 & \sqrt{\frac{1}{2}} & & & & & \\ \sqrt{\frac{1}{2}} & 0 & \sqrt{\frac{2}{2}} & & & & \\ & \sqrt{\frac{2}{2}} & 0 & \sqrt{\frac{3}{2}} & & & \\ & & \ddots & \ddots & \ddots & & \\ & & & \ddots & \ddots & 0 & \sqrt{\frac{n-1}{2}} \\ & & & & & \sqrt{\frac{n-1}{2}} & 0 \end{pmatrix}, \tag{6}$$

which are symmetrically distributed about the origin.

In Sec. 2 we employ the Leverrier-Takeno's technique [18] to realize applications of (2, 4, 6).

SOME APPLICATIONS OF THE COHEN'S RESULTS

The characteristic equation of a matrix $\boldsymbol{A}_{n\,x\,n}$:

$$\lambda^n + a_1\,\lambda^{n-1} + a_2\,\lambda^{n-2} + \cdots + a_n = 0, \tag{7}$$

can be constructed via the Leverrier-Takeno's procedure:

$$a_1 = -s_1\,, \qquad a_2 = \frac{1}{2}[(s_1)^2 - s_2], \qquad a_3 = \frac{1}{6}[-(s_1)^3 + 3s_1\,s_2 - 2s_3],\ \ldots \tag{8}$$

where s_r is the trace of $\boldsymbol{A}^r$. Then we consider (2):

$$\boldsymbol{P}_2 = \begin{pmatrix} 0 & \frac{1}{\sqrt{3}} \\ \frac{1}{\sqrt{3}} & 0 \end{pmatrix}, \qquad \boldsymbol{P}_2^2 = \begin{pmatrix} \frac{1}{3} & 0 \\ 0 & \frac{1}{3} \end{pmatrix}, \qquad s_1 = a_1 = 0, \quad s_2 = \frac{2}{3}\,, \quad a_2 = -\frac{1}{3}\,,$$

thus (7) implies the equation $3\lambda^2 - 1 = 0$ in agreement with $P_2(x) = 0$. Similarly:

$$\boldsymbol{P}_3 = \begin{pmatrix} 0 & \frac{1}{\sqrt{3}} & 0 \\ \frac{1}{\sqrt{3}} & 0 & \frac{2}{\sqrt{15}} \\ 0 & \frac{2}{\sqrt{15}} & 0 \end{pmatrix}, \qquad \boldsymbol{P}_3^2 = \begin{pmatrix} \frac{1}{3} & 0 & \frac{2}{3\sqrt{5}} \\ 0 & \frac{3}{5} & 0 \\ \frac{2}{3\sqrt{5}} & 0 & \frac{4}{15} \end{pmatrix}, \qquad \boldsymbol{P}_3^3 = \begin{pmatrix} 0 & \frac{\sqrt{3}}{5} & 0 \\ \frac{\sqrt{3}}{5} & 0 & \frac{6}{5\sqrt{15}} \\ 0 & \frac{6}{5\sqrt{5}} & 0 \end{pmatrix},$$

Hence, $s_1 = a_1 = 0$, $s_2 = \frac{6}{5}$, $a_2 = -\frac{3}{5}$, $s_3 = a_3 = 0$, and from (7) we obtain $5\lambda^3 - 3\lambda = 0$ in harmony with $P_3(x) = 0$. Let's remember that the roots of Legendre polynomials are important in the Gaussian quadrature [7], in the study of electromagnetic radiation and the angular function for the hydrogen atom.

Besides, from (4):

$$\boldsymbol{L}_2 = \begin{pmatrix} 1 & 1 \\ 1 & 3 \end{pmatrix}, \qquad \boldsymbol{L}_2^2 = \begin{pmatrix} 2 & 4 \\ 4 & 10 \end{pmatrix}, \qquad s_1 = 4, \quad s_2 = 12, \quad a_1 = -4, \quad a_2 = 2,$$

then (7) gives $\lambda^2 - 4\lambda + 2 = 0$, equivalent to $L_2(x) = 0$; and:

$$\boldsymbol{L}_3 = \begin{pmatrix} 1 & 1 & 0 \\ 1 & 3 & 2 \\ 0 & 2 & 5 \end{pmatrix}, \qquad \boldsymbol{L}_3^2 = \begin{pmatrix} 2 & 4 & 2 \\ 4 & 14 & 16 \\ 2 & 6 & 29 \end{pmatrix}, \qquad \boldsymbol{L}_3^3 = \begin{pmatrix} 6 & 18 & 18 \\ 18 & 78 & 108 \\ 18 & 108 & 177 \end{pmatrix},$$

therefore $s_1 = 9,\ s_2 = 45,\ s_3 = 261,\ a_1 = -9,\ a_2 = 18,\ a_3 = -6,$ and from (7) we deduce that $\lambda^3 - 9\lambda^2 + 18\lambda - 6 = 0$ in according with (3). The Laguerre polynomials participate in the radial function of hydrogen-like atoms [19] and diatomic molecules [20].

For the Hermite polynomials, we have:

$$\boldsymbol{H}_2 = \begin{pmatrix} 0 & \sqrt{\frac{1}{2}} \\ \sqrt{\frac{1}{2}} & 0 \end{pmatrix}, \qquad \boldsymbol{H}_2^2 = \begin{pmatrix} \frac{1}{2} & 0 \\ 0 & \frac{1}{2} \end{pmatrix}, \qquad s_1 = a_1 = 0,\ s_2 = 1,\ a_2 = -\frac{1}{2},$$

implying the characteristic equation $2\lambda^2 - 1 = 0,$ equivalent to $H_2(x) = 0$; and:

$$\boldsymbol{H}_3 = \begin{pmatrix} 0 & \sqrt{\frac{1}{2}} & 0 \\ \sqrt{\frac{1}{2}} & 0 & 1 \\ 0 & 1 & 0 \end{pmatrix}, \qquad \boldsymbol{H}_3^2 = \begin{pmatrix} \frac{1}{2} & 0 & \sqrt{\frac{1}{2}} \\ 0 & \frac{3}{2} & 0 \\ \sqrt{\frac{1}{2}} & 0 & 1 \end{pmatrix}, \qquad \boldsymbol{H}_3^3 = \begin{pmatrix} 0 & \frac{3}{2}\sqrt{\frac{1}{2}} & 0 \\ \frac{3}{2}\sqrt{\frac{1}{2}} & 0 & \frac{3}{2} \\ 0 & \frac{3}{2} & 0 \end{pmatrix},$$

$s_1 = a_1 = 0,\ s_2 = 3,\ a_2 = -\frac{3}{2},\ s_3 = a_3 = 0,$ thus (7) gives the expression $2\lambda^3 - 3\lambda = 0$ which is compatible with $H_3(x) = 0.$ The Hermite polynomials are fundamental in the analysis of the harmonic oscillator in quantum physics.

Thus we have that the Leverrier-Takeno's process [18] allows to see that the eigenvalues of the matrices (2, 4, 6) are the roots of the Legendre, Laguerre [21, 22], and Hermite polynomials, respectively. Let's remember that the QR algorithm [23-26] is an efficient method to determine the proper values of a matrix.

REFERENCES

A. Bucur, B. E. Carvajal-Gámez, J. López-Bonilla, *Laguerre polynomials: Their Laplace transform via equidistant interpolation,* J. Sci. Res. **53** (2009) 257-258.

A. M. Cohen, *An algebraic approach to certain differential eigenvalue problems,* Linear Algebra and its Appls. **240** (1996) 183-198.

A. M. Cohen, *Numerical methods for Laplace inversion,* Springer, New York (2007).

C. Lanczos, *Applied analysis,* Dover, New York (1988).

D. S. Watkins, *The QR algorithm revisited,* SIAM Rev. **50** (2008) 133-145.

E. R. Smith, *Zeroes of the hermitean polynomials,* Am. Math. Monthly **43** (1936) 354-358.

F. Pidduck, *Laguerre polynomials in quantum mechanics,* J. London Math. Soc. (1) **4** (1929) 163-166.

G. Golub, F. Uhlig, *The QR algorithm: 50 years later its genesis by John Francis and Vera Kublanovskaya and subsequent developments,* IMA J. Numer. Anal. **29**, No. 3 (2009) 467-485.

H. E. Salzer, R. Zucker, R. Capuano, *Table of the zeros and weight factors of the first twenty Hermite polynomials,* J. Res. Nat. Bureau Stand. **48**, No. 2 (1952) 111-116.

http://mathworld.wolfram.com/Laguerre-GaussQuadrature.html

https://math.stackexchange.com/questions/104845/the-roots-of-hermite-polynomials-are-all-real

I. Guerrero-Moreno, J. López-Bonilla, J. Rivera-Rebolledo, *Leverrier-Takeno coefficients for the characteristic polynomial of a matrix,* J. Inst. Eng. **8**, No. 1-2 (2011) 255-258.

J. H. Caltenco, J. López-Bonilla, J. Rivera-Rebolledo, *Gaussian quadrature via Hermite and Lagrange interpolations,* J. Sci. Res. **55** (2011) 177-180.

J. G. F. Francis, *The QR transformation: A unitary analogue to the LR transformation,* The Computer Journal **4**, No. 3 (1961) 265-271 and 332-345.

J. H. Caltenco, J. López-Bonilla, R. Peña-Rivero, *Morse's radial wave function,* Lithuanian J. of Phys. **50**, No. 4 (2010) 403-404.

J. López-Bonilla, A. Lucas-Bravo, S. Vidal-Beltrán, *Integral relationship between Hermite and Laguerre polynomials: Its application in quantum mechanics,* Proc. Pakistan Acad. Sci. **42**, No. 1 (2005) 63-65.

J. López-Bonilla, B. Man Tuladhar, R. Peña-Rivero, *Relationship between wave functions of two-dimensional hydrogen atom in parabolic and polar coordinates,* J. Sci. Res. **54** (2010) 219-22.

J. López-Bonilla, R. López-Vázquez, H. Torres-Silva, *On the Legendre polynomials,* Prespacetime Journal **6**, No. 8 (2015) 735-739.

J. López-Bonilla, G. Posadas-Durán, *On the Saha's generating function for the Hermite polynomials,* Prespacetime Journal **7**, No. 13 (2016) 1805-1806.

J. López-Bonilla, R. López-Vázquez, V. M. Salazar del Moral, *On some identities for the Laguerre polynomials,* Prespacetime Journal **8**, No. 10 (2017) to appear.

J. Mawhin, A. Ronveaux, *Schrödinger and Dirac equations for the hydrogen atom, and Laguerre polynomials,* Arch. Hist. Exact Sci. **64** (2010) 429-460.

R. Cruz-Santiago, J. López-Bonilla, S. Yáñez-San Agustín, *A note on the Laguerre polynomials,* Prespacetime Journal **8**, No. 4 (2017) 511-512.

R. E. Greenwood, J. J. Miller, *Zeros of the Hermite polynomials and weights for Gauss mechanical quadrature formula,* Bull. Am. Math. Soc. **54**, No. 8 (1948) 765-769.

V. Barrera-Figueroa, J. López-Bonilla, J. Sosa, *Multiple root finder algorithm for Legendre and Chebyshev polynomials via Newton's method,* Annales Mathematicae et Informaticae **33** (2006) 3-13.

V. Barrera-Figueroa, J. López-Bonilla, J. Sosa, *Method of moments and non-uniform sampling via Legendre polynomials roots,* Bol. Soc. Cub. Mat. Comp. **7**, No. 1 (2009) 19-33.

V. N. Kublanovskaya, *Certain algorithms for the solution of the complete eigenvalue problem,* Soviet Math. Dokl. **2** (1961) 17-19.

RELATIONSHIP BETWEEN WATER QUALITY & BLACK FLIES (DIPTERA: SIMULIIDAE) ABUNDANCE IN TAMBUNAN DISTRICT, SABAH.

Nur Ashiqin Abdul Hamid[1*], Maria Lourdes T. Lardizabal[1], Hiroyuki Takaoka[2], Estherpeni Stephen[1] & Maznah Mahali

[1]Faculty of Science and Natural Resources, University Malaysia Sabah, Jln. UMS, 88400 Kota Kinabalu, Sabah, Malaysia
[2]Institute of Biological Sciences, Faculty of Science, University of Malaya, 50603 Kuala Lumpur
Corresponding author: Nur Ashiqin Abudul Hamid
Email: ashiqinhamid@gmail.com

ABSTRACT. *A study to investigate the relationship between black flies (Simuliidae) pupa abundance and physio-chemical parameters such as velocity, water temperature, pH, dissolved oxygen, conductivity and total dissolved solid was conducted at Tambunan district, Sabah. A total of six rivers were selected as sampling stations. Five sampling points located at a distance of 5-10 meters were established in each sampling station. Sampling was conducted every fortnight for a duration of six months from October 2015 until March 2017. Samples of black flies larvae and pupae were manually collected from substrates consisting of grasses, plant roots and plastics which were found stuck in between the rocks with running water area. Water quality parameters that were measured during every sampling, include water temperature, velocity, pH, dissolved oxygen, conductivity and total dissolve solids (TDS). Results from this study showed that The Principal Component Analysis (PCA) revealed two PC's which had eigenvalues >1.0 and together accounted for 78% total variability of the physio-chemical parameters. PC-1 which accounted 56% of variability defined a normal temperature (23-25^{0}C), high water velocity, high dissolved oxygen, low conductivity and low total dissolved solid. While PC-2 explained 22% of the variability was related to water pH. Pearson's correlation result shows that only velocity had a significant relationship with the abundance of black flies ($r=0.512$, $p<0.01$), while other parameters did not show any significant relationship with its abundance. In conclusion, results from this study revealed that only water velocity had a significant relationship with the abundance of black flies.*

KEYWORDS: Black flies, physio-chemical parameters, Tambunan.

INTRODUCTION

Black flies (Diptera: Simuliidae) are among the best-known aquatic insect in resource turnover and have been extensively studied worldwide. Black flies belong to the Order diptera and family Simuliidae (Zhang *et al.*, 1998). Their populations are distributed widely in Africa, America and some Asian countries such as India, Japan and South-East Asia (Srisuka *et al.*, 2015; Adler, 2005; Butler *et al.*, 1998). Immature black flies (larvae and pupa) prefer running water habitat which contains high oxygenated concentration in

waterways such as rivers, streams and waterfalls (Craig, 2003). Such habit makes the black flies important to the lotic ecosystem either for their integral role in organic matter processing in streams (Hart, 1986) or as a prey for food web dynamic in the lotic ecosystems (Cummins, 1988). According to Vincent & John (1975), *Simulium* is the first insect that appears in the recovery zone, which makes this insect group one of suitable bio-indicators for water quality. Some species are often found only in clean water, while some species can adapt to polluted water and these species are distributed in a wide range of ecological tolerances (Hamada & Grillet, 2001; Vincent & John, 1975).

On the contrary, some species of blackflies have been reported as disease vectors of river blindness' and skin problems in some countries such as in North America and Africa (Adler *et al*., 2004). This is caused by the adult females of these insects which are serious blood feeders that can cause the disease (Creadie *et al.*, 2011; Catherine *et al.*, 2010).

Black flies are less known in Malaysia and ecological research about this aquatic insect is still inadequate especially in the Borneo region (Takaoka, 1996; Takaoka, 2008). Most of the earlier studies on black flies in Sabah were related to taxonomy. Studies on the ecology and role of black flies as bio-indicator had so far not been well reported yet. Therefore, the aim of this study was to determine whether there is any relationship between black flies (Simuliidae) pupa abundance and the water quality.

MATERIALS AND METHODS

Study area: This study was conducted from October 2015 until March 2016. Black flies pupae and larvae were sampled once every fortnight which resulted 12 sampling efforts throughout the six months duration. Sampling stations were located in six selected rivers within the Tambunan district, Sabah. Habitat characterization and location of the rivers were as listed in Table 1.

Sampling procedure : At each sampling station, larvae and pupae were manually collected from all types of substrates that includes leaf litter, rocks, twigs and the artificial substrates such as plastics that are usually found stuck in between rocks in running water area at depths less than 100 cm (Figure 1). The river was chosen based on methods adapted from Zubaidah *et al.* (2016). Characteristics for choosing the streams would include the convenience of accessibility for sampling, the presence of substrates and continuous water flow. Five sampling points along the stream was set up at each site. The distance between sampling points ranged between 5-10 meters from each point (Figure 2). Sampling of pupae and larvae was conducted for about thirty minutes at each station. Physio-chemical parameters were also recorded during the sampling at each station. *In-situ m*easurement of the physio-chemical water quality was taken by using multi-parameter probe EUTECH PCD-650 for dissolve oxygen (DO), pH, conductivity, temperature and total dissolve solid (TDS).

Samples of black flies larvae and pupae were removed from the substrate and stored in eppendorf tubes containing 80% ethanol for preservation and identification. At the laboratory, mature pupae of black flies were sorted and placed into vials until the adult black flies emerged. Emerged adult black flies along with its pupae skin were preserved in eppendorf vials which contain 80% alcohol for further identification. Specimens of black flies were identified based on taxonomic key references (Takaoka 2001; Takaoka *et al.*, 2012).

Table 1: Habitat characterization of study areas.

Stations	GPS Location	Depth (m)	Width (m)	Habitat Description
Sg. Kerokot	N05°49'33.1"E116°29'39.5"	0.4	6.33	Fast flowing water, rocky bottom. Open canopy
Sg Lumondou	N05°42'54.7" E116°24'08.8"	0.45	7.67	Fast flowing water, rocky bottom. Open canopy.
Sg. Pegalan	N05°42'47.1" E116°24'28.2"	0.60	0.62	Fast flowing water, rocky bottom. Open canopy.
Sg. Tambunan	N05°41'42.6" E116°22'57.4"	0.15	1.33	Moderate water current, rocky and sandy bottom. Open canopy.
Sg. Malungung	N05°37'35.2" E116°17'12.7"	0.27	2.75	Fast flowing water, rocky bottom. Open canopy.
Sg. Kinabaan	N05°43'46.9" E116°23'27.5"	0.22	3.42	Moderate current, gravelly and rocky bottom. Open canopy

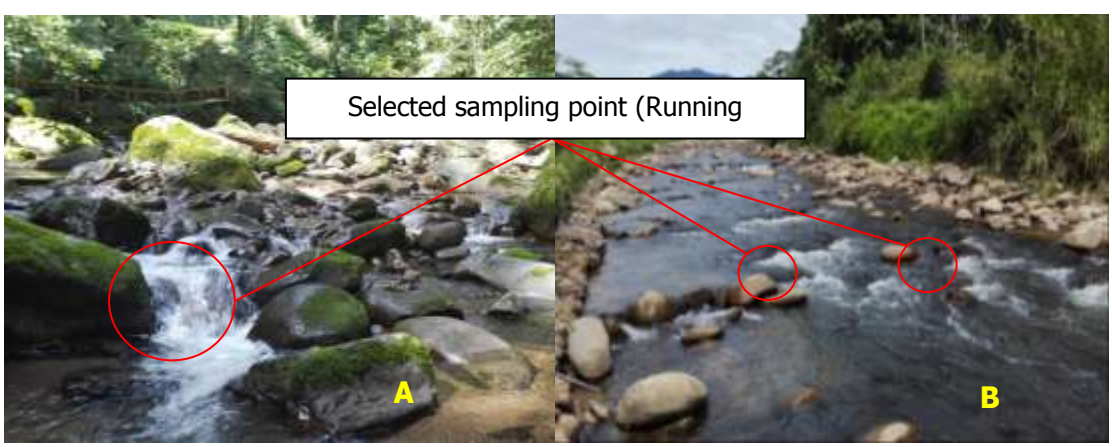

Figure 1: Running water area for black flies to breed. A) Sg Mahua, B) Sg Lumondou.

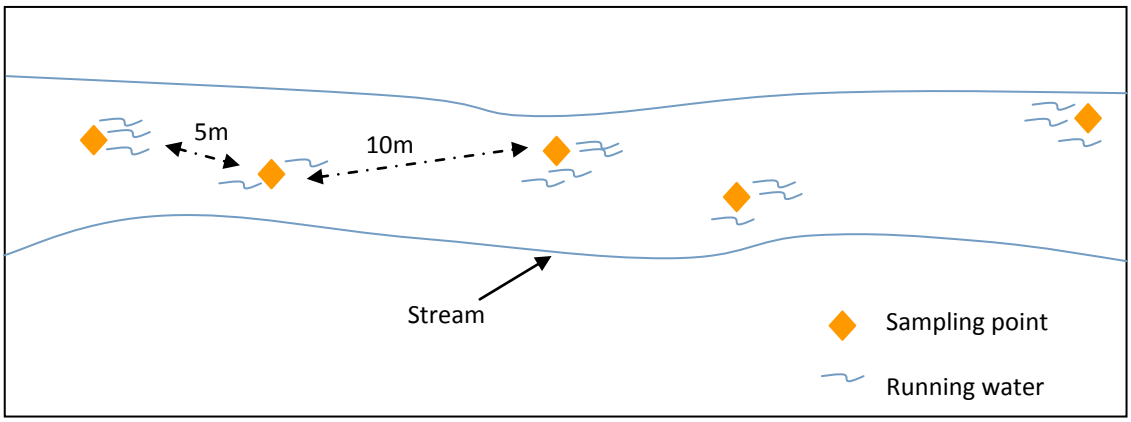

Figure 2: Distances of sampling points were set up at running water area.

Data Analysis : Diversity indices such as Shannon Weiner (H), Dominance (D) and species richness was analyzed with the aid of PAST version3 software (Srisuka *et al.*, 2015). Principal Component Analysis (PCA) was used to determine which combination of physio-chemical parameters were more predictive in describing each parameters which are velocity, water temperature, water pH, dissolved oxygen, total dissolve oxygen and conductivity (Scheiber & Debandi, 2008). The PCA was also used to reduce the number of parameters into groups of independent components (Zubaidah *et al.*, 2016). Spearman Correlation was used to determine the relationship between the principal component (PC) and the abundance of black flies (Zubaidah *et al.*, 2016). Pearson's correlation coefficient (r) was used to determine the interdependence of the physio-chemical parameters, whether the parameters (velocity, water temperature, water pH, dissolved oxygen, total dissolve oxygen and conductivity) were correlated each other and with the abundance of black flies (Popoola & Otalekor, 2011). All tests were considered significant at $p<0.01$. Water quality classification was referred based on the Water Quality Index Classification by Department of Environmental (DOE, 2006).

RESULTS AND DISCUSSIONS

A total of 8107 individual (pupa) of black flies were collected from October 2015 until March 2016. Throughout the sampling period, a total of seven black flies species were recorded. Figure 3 showed the diversity index for the six sampling stations in Tambunan. Diversity index values ranged between 0.04 and 1.3 which indicated a low diversity of black flies in the sampling stations. The highest Shannon Weiner (H) diversity index value was 1.3 that was recorded at Sg Tambunan. There were seven species of black flies recorded in Sg Tambunan, namely, *S. sabahense, S.beludense, S. keningauense, S. parahiyangum, S. sp, S. sheilae* and *S. aureohirtum*. Meanwhile, the lowest index value was 0.04 at Sg Lumondou with four species of black flies recorded which are *S. sabahense, S.beludense, S. keningauense,* and *S. parahiyangum,*. The highest dominance index was recorded in Sg Lumondou with the index value of 0.98, indicating the presence of a dominant species. The dominant species that recorded at this site was *S. beludense.*

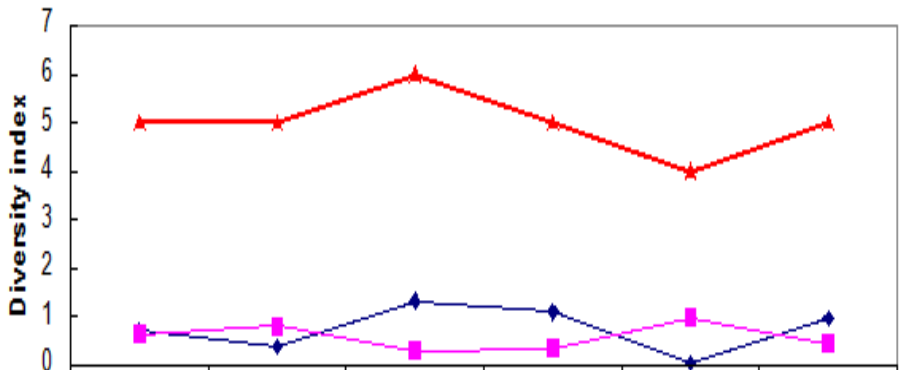

	Sg Kinabaan	Sg Kerokot	Sg Tambunan	Sg Malungung	Sg Lumondou	Sg Pegalan
Shannon_H	0.7268	0.3874	1.321	1.097	0.04397	0.9658
Dominance_D	0.6553	0.8154	0.3154	0.3513	0.9877	0.4507
Species Richness	5	5	6	5	4	5

Figure 3: Diversity index value for black flies at selected streams in Tambunan.

Sg. Lumondou recorded the highest abundance of black flies pupae (2918 individual; 36% total abundance), while Sg. Tambunan recorded the lowest pupae abundance with 191 individuals (2.35% total abundance) of pupae (Table 2). Among the seven species recorded, *Simulium sabahense* and *Simulium beludense* (Figure 3) were recorded as a common species found at all the sites (Table 3). For this study, immature black flies from the species *S. sabahense, S.beludense, S. keningauense, S. parahiyangum* and *S. aureohirtum* was highly abundant in running water area with the water current velocity between 0.3 to 0.5 m/sec and range of river width of 3-6 m. While, *S. Sheilae* was found only at Sg Tambunan which has slow-flowing water velocity of 0.1-0.2 m/sec, and a similar finding was also reported by Takaoka (2001).

Table 2: Abundance of individual black flies and mean water quality parameter

Stations	N (Total pupa)	Abundance (%)	Velocity (m/sec)	DO (%)	pH	TDS (ppm)	Conductivity (µS/cm)	Temp (°C)	River Classification (DOE,2006)
S1	191	2.35	0.2±0.15	82.7±3.32	6.83±0.24	125.3±9.59	127.5±10.1	24.2±1.47	Class I (Notes : Class I – Conservation of natural environment; Water Supply I – practically no treatment (only boiling needed) Fishery I – very sensitive (aquatic)
S2	347	4.28	0.2±0.15	88.7±1.05	6.87±0.32	75.85±8.39	81.9±8.92	24±1.21	
S3	610	7.25	0.44±0.19	85.6±3.21	6.6±0.32	52.15±10.4	55.61±10.9	21.1±0.3	
S4	1275	15.73	0.2±0.55	85.8±2.61	6.7±0.26	40.9±15.01	35.2±15.03	22.2±0.82	
S5	2766	34.12	0.29±0.18	84.1±3.25	6.76±0.36	101.8±15.0	112.4±18.4	24±0.76	
S6	2918	35.99	0.36±0.28	82.8±3.90	6.68±0.33	63.87±9.22	61.94±8.79	23.6±1.5	

S1: Sg Tambunan; S2: Sg. Kinabaan; S3: Sg. Kerokot; S4: Sg. Pegalan; S5: Sg.Malungung; S6: Sg.Lumondou

Table 3: Composition and distribution of black flies at the sampling stations in Tambunan District, Sabah

Subgenus/ Species	Sg.Kerokot	Sg. Lumondou	Sg. Pegalan	Sg. Malungung	Sg. Tambunan	Sg.Kinabaan
Subgenus : *Simulium*						
S.sabahense	+	+	+	±	+	+
S.kemingawense	+	+	+	+	+	+
S.aureohirtum	-	-	-	-	+	+
Gomphostilbia						
S.beludense	±	±	+	±	+	±
S.parahyangum	+	+	+	+	+	+
S.sheilae	+	-	+	+	+	-

+: Present; ±: Common; -: absent

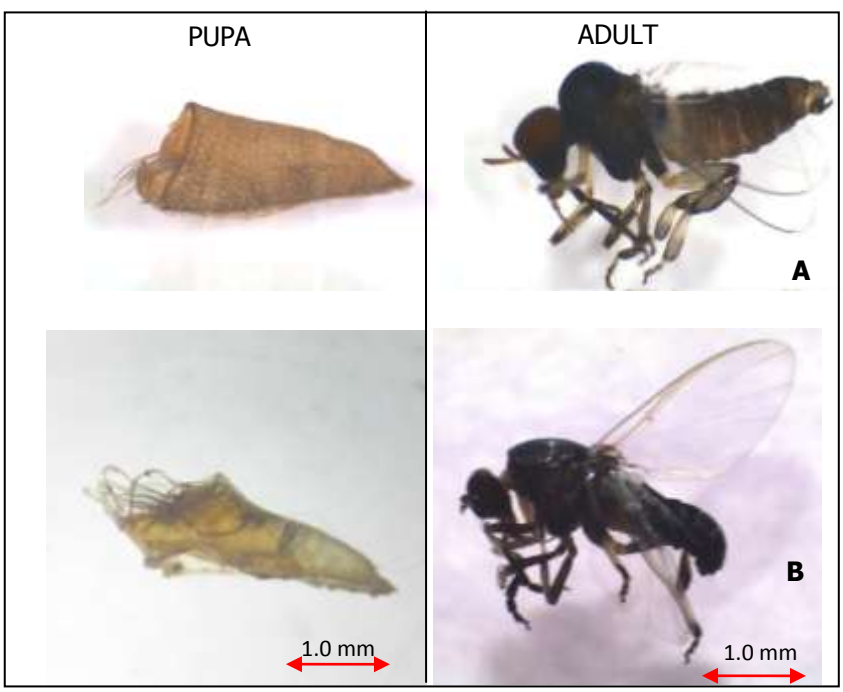

Figure 4: The common black flies species recorded A) *S. sabahense*, B) *S.beludense.*

Physiochemical parameter

Principal Component Analysis (PCA) of physio-chemical properties revealed two PC's (Figure 5), which have eigenvalue >1.0 with 78% total variance of the physio-chemical parameters (Table 4). PC-1 accounted 56% of variability, which was derived mostly from velocity, temperature, dissolved oxygen, conductivity and TDS. While PC-2 explained 22% of the variability was related to water pH. The sites with higher PC-1 were at normal temperature (23-25^{0}C), high water velocities, high dissolved oxygen, low conductivity and low total dissolved solid.

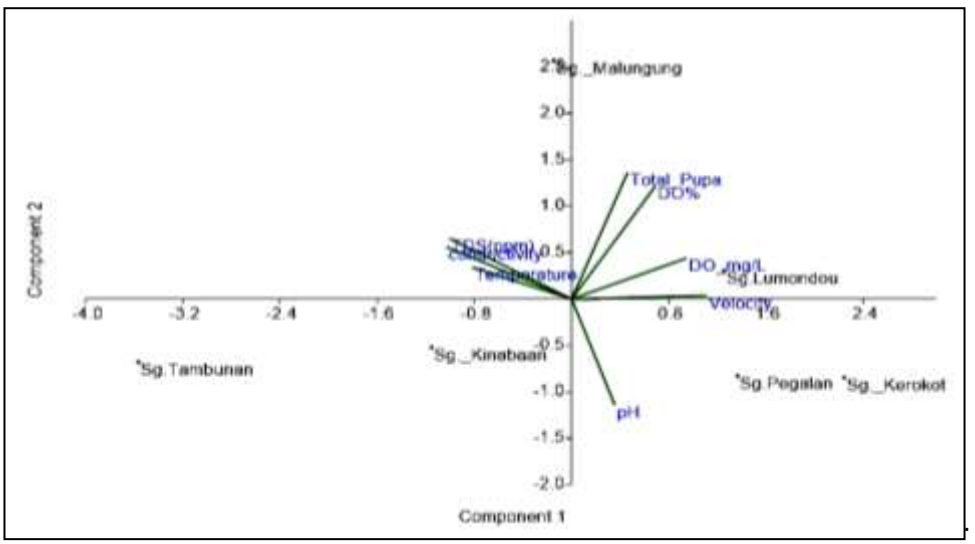

Figure 5: Biplot of sampled sites and physio chemical parameters resulting from PCA.

Result from PC-1 shows that velocity, temperature, dissolved oxygen, conductivity and TDS were associated with the black flies abundance. Previous findings showed the importance of water velocity for black flies distribution (Zubaidah *et al.*, 2016; Srisuka *et al.*, 2015). This is because the running water usually provides a good aeration, which also influenced the dissolved oxygen. According to Doisy *et al.* (1986), black flies larvae require at least 78% saturation of dissolve oxygen, while some species require between 92 to 98% of saturation.

Table 4: PCA and Spearman's rank coefficient of physio-chemical parameter in Tambunan.

Parameters	**Min - Max**	**Mean ± STD**	**PC1**	**PC2**
Velocity (ms^{-1})	0.3 - 0.7	0.62 ± 0.14	**0.988***	0.021
Temperature (^oC)	21 - 26	24.47 ± 1.76	**-0.729***	0.190
pH	7.21 - 7.29	7.25 ± 0.03	0.316	**-0.636****
Conductivity (μs^{-1})	63 - 119	96.92 ± 30.74	**-0.918****	0.313
Total Dissolved Solid (ppm)	58.4 - 134	91.39 ± 29.56	**-0.896****	0.363
Dissolved Oxygen (mg/L)	6.6 - 7.3	6.94 ± 0.29	**0.843***	0.245
Eigenvalues			4.5	1.7
% Proportion			56.39	22.05
Cumulative			56.39	78.44

*p<0.01, **p<0.001

Water temperature was also reported as one of the most important parameter that influenced the aquatic insect distribution (Scheibler & Debandi, 2008). The range of water temperature for this study was from 21^{o}C-26 ^{o}C. TDS and conductivity also influenced the abundance of black flies pupa, this is because there was a change of weather during the sampling period. The changes of weather may affect the condition of water against the total dissolve solids and conductivity (Laurince & Philippe, 2013). In this study the value of conductivity and TDS fluctuated due to the weather changed, and there was flood during the sampling. The higher value of TDS and conductivity was due to soil erosion caused by heavy rain. PC-2 showed pH as the only parameter which had negative relationship to the black flies distribution. For this study, the range of pH value was from 7.21 to 7.29.

Pearson's correlation coefficient (r) showed the relationship between the physio-chemical parameters and total pupa recorded at sampling sites (Table 5). The result showed that only velocity had a significant relationship with the total pupa ($r=0.52$, $p<0.01$), while other parameters did not show a significant relationship. The analysis showed that water velocity had a significant relationship with dissolved oxygen ($r=0.512$, $p=0.004$) and water pH ($r=-0.58$, $p=0.007$). The water velocity had moderate and positive correlation with dissolved oxygen, which meant that the higher the water velocity, the higher would be the saturation of dissolved oxygen. While other parameters such as pH, temperature, conductivity and TDS had inverse correlation with velocity. The temperature value recorded during the sampling period ranged between 21^{o}C to 24^{o}C, which were in the optimal range of tropical fresh waters (Popoola & Otalekor, 2011).

Pearson's correlation showed that water temperature had a strong relationship with dissolved oxygen (r=-0.84, p=0.04). Water velocity also was correlated negatively with conductivity and TDS. Pearson's correlation analysis showed that conductivity had a strong and positive correlation with TDS (r=0.93, p=0.003). Both conductivity and TDS indicated the presence of ions concentration that determined the quality of water (Tariq *et al*., 2006). Therefore, high water velocity may also decrease the source of dissolve ions in the water as in Siddaramu & Puttaiah (2013).

Table 5: Pearson's correlation (r) values between the physio-chemical parameters.

Parameters	Total Pupa	Velocity (ms^{-1})	pH	Temperature (^0C)	Conductivity (μs^{-1})	TDS (ppm)	Dissolve Oxygen (%)
Total Pupa	**1**						
Velocity	0.524*	**1**					
pH	-0.286	-0.581*	**1**				
Temperature	0.522	-0.502	0.227	**1**			
Conductivity	0.065	-0.560	0.065	-0.062	**1**		
TDS(ppm)	-0.084	-0.607	-0.098	0.060	0.929*	**1**	
DO%	0.516	0.512*	0.057	-0.844*	-0.313	-0.417	**1**

*p<0.01

From this study, all six selected rivers were classified as Class 1 river according to Water Quality Index Classification (DOE, 2006). From this study, all six selected rivers were classified as Class 1 rivers according to the Classification of Water Quality Index (DOE, 2006). Characteristics of a Class 1 river has a conserved natural ecosystem, practically no water treatment is required for water supply and sensitive aquatic species that exist in the river.

Limitations of this study had included the unpredictable change of weather that affected the sampling activities especially during rainy seasons. Heavy rain that caused flooding and high water current velocity washed away the substrates, thus leaving very little available substrates to sample. In addition, there were more potential stations around Tambunan, but some rivers were being restricted due to the "tagal" system in Sabah which thus makes the river inaccessible without the permission of the village chief.

CONCLUSIONS

As a conclusion, there were seven species of black flies recorded in this study. The dominant species at all study sites were *S. sabahense* and *S. beludense* , and results from the diversity index that ranged between 0.04 and 1.3 indicated that the diversity of black flies in Tambunan was still low. Findings from this study also showed that only water velocity had a significant relationship ($r=0.52$, $p<0.01$) with the black flies abundance. It is thus recommended that in-depth study on black flies habitat preferences, vertical and horizontal distribution of black flies should be done in the future to deepen the knowledge on ecology and biology of the different black flies species.

ACKNOWLEDGEMENT

This study was funded by SGPUMS Research Grant (UMS/SBK107-STWN-2013). We would also like to express our gratitude to the Ministry of Education for granting MyBrain15 (MyMaster). Special thanks also to the expertise from University Malaya (UM), Prof Hiroyuki Takaoka for helping in the identification of black flies species and also to Prof Dato'. Dr Mohd. Sofian bin Azirun and Dr. Chen Chee Dang for ideas and advises. Last but not least, our special appreciation to the Sabah Parks management for granting us the permission and research permit to conduct this study within the Kinabalu Park and Crocker Range Park area. Not forgetting also all staff of Kinabalu Parks who had rendered their guidance during our field sampling in the park areas.

REFERENCES

Adler, P.H., Currie, D.C., & Wood, D.M. (2004). The Black flies (Simuliidae) of North America. ROM Publication in Sciences, New York, NY

Adler, P. H. (2005). Black flies, the Simuliidae. In W. C. Marquardt (ed.).Biology of DiseaseVectors, 2nd edition. *Elsevier Academic Press*, San Diego. 127-140 pp.

Butler, J.F & Hogsette, J A. (1998). Blackflies. Simulium spp.(Insecta:Diptera:Simuliidae). University of Florida, IFAS Extension,EENY-030. Retrieved 23th November 2015.(http://entomolpgy.ifas.ufl.edu).

Catherine A.H, Jessica P & John F. (2010). Black Flies : Biology and Public Health Risk Department of Entomology. Purdue University, E-251-W.

Cummins, K.W. (1988). The functional role of black flies in stream ecosystems,pp.1-10. In Kim, K.C. & Merrit, R.W (eds) Black flies : *Ecology, Population Management, and Annotated World List*. Pennslvania State University, University Park, P.A.

Craig, D.A. (2003). Geomorphology, Development of Running Water Habitats, and Evolutiuon of Black flies on Polynesian Islands. *BioScience*. **53** (11):1079-1093 pp.

Creadie, J.W., Adler, P.H & Beard, C.E. (2011). Ecology of Symbiotes of Larval Blackflies (Diptera: Simuliidae): Distribution, Diversity and Scale. EntomologicalSociety of America. *Environmental Entomology.* **40** (2): 259-302 pp.

Department of Environment. (2006). *Malaysia Environmental Quality Report*. Ministry of Natural Resources and Environment Malaysia, Kuala Lumpur. 86 pp.

Doisy, K.E, Hall, R.D. & Fischer, F.J. (1986). The Black flies (Diptera: Simuliidae) of an Ozark Stream in South Missouri and Associated Water Quality Measurement. *Journal of The Kansas Entomology Society*. **59** (1): 133-142 pp.

Hamada, N., & Grillet, M. E. (2001). Black flies (Diptera :Simuliidae) of the Gran Sabana keys for larvae and pupae, **16** (1):29-49 pp.

Hart, D.D. (1986). The Adaptive Significant of Territoriality in Filter-Feeding Larval Blackflies (Diptera:Simuliidae).*Oikos,* Vol. **46**, (1): 88-92 pp.

Laurince, M. Y., Celestin, B. A & Philippe, K. (2013). Composition, abundance and diversity of aquatic insects in fishponds of southern Ivory Coast, West Africa. *FaunisticEntomology.* **66**:123-133 pp.

Popoola, K. O. K & Otalekor, A. 2011. Analysis of Aquatic Insect's Community of Awba Reservoir and its Physio-chemical Properties. *Journal of Environmental and Earth Science.* **3**(4):422-428 pp. Scheibler, E. E., & Debandi, G. O. 2008. Spatial and Temporal patterns in the aquatic community of high altitude Andean stream (Mendoza, Argentina). *Aquatic Insect.Taylor and Francis Group*. **30** (2): 145-161

Siddaramu, D & Puttaiah, E.T. (2013). Physiochemical characteristic of Balagala Kere and Purali Kere of Shimoga District, Karnataka, India. *International Journal of Advanced Research*. **1** (8):313-321pp.

Srisuka, W. Takaoka. H, Yatsushi, O. Masako. F, Sorawat. T, Kristsana. Y, Wej. C, Atiporn, S. 2015.Seasonal biodiversity of black flies (Diptera: Simuliidae) and evaluation of ecological factor influencing species distribution at Doi Pha Hom Pok National Park, Thailand. Elsevier. 149: 212-219.

Takaoka, H. (2001). Two new and three newly recorded species of Black flies(Diptera: Simuliidae) in Sabah, Malaysia.*Japanese Journal of Tropical Medicine and Hygiene*. **29:** 111 114 pp. Takaoka, H. (2008). Taxonomic revision of *tuberosum* species-group of Simulium (Simulium) in Sabah and Sarawak, Malaysia (Diptera:Simuliidae). *Med Entomology and Zoology*. **59** (2):55-80 pp.

Takaoka, H., Sofian, M.A. Rosli, H. Yasushi, O. Daicus, M.B. & Tan, P.E. (2012). Relationships of Black fly species of the *Simulium tuberosum* species group (Diptera: Simuliidae) in Peninsular Malaysia, with keys to ten Malaysia Species. *The Raffles Bulletin of Zoology.* **60** (2): 533-538 pp.

Takaoka, H. (1996). Description of a new species of *Simulium (Simulium)* from Sabah, Malaysia (Diptera :Simuliidae). *Journal of Japan Medical Zoology.* **24** (3). 157-161 pp.

Tariq, M. , Ali, M & Shah, Z. (2006). Characteristic of industrial effluents and their possible impacts on quality of underground water. *Soil & Environment*. **25** (1) :64-49pp.

Vincent, H., & John, D. 1975. Water Quality Monitoring and Aquatic Organism: The Importance of Species Identification. Vol. (47).No 1, pp.9-19

Zhang, Y., Malmqvist, B. & Englund, G. (1998). Ecological processes affecting community structure of black fly larvae in regulated and unregulated rivers. *Journal of Applied Ecology*, 35: 678-686 pp.

Zubaidah, Y. Takaoka, H. Pramual, P. Low, V.L. & Sofian, A.M. 2016. Breeding habitat preference of preimaginal black flies (Diptera: Simuiidae) in Peninular Malaysia. *Acta Tropica, Elsevier.* 153: 57-63.

INSTRUCTIONS TO CONTRIBUTORS / AUTHOR

Manuscripts
The official language of the Journal is English but papers may also be submitted in Bahasa Malaysia (with an English abstract). All manuscripts should be submitted in duplicate to the Editor-in-Chief, typed on one side of good quality A4 paper, double spacing with a wide margin. The S.I. unit system should be used throughout. Submission of an article is understood to imply that the article is original, unpublished and is not considered for publication elsewhere.

The manuscript should be arranged in the following order: title page, abstract (short communications require no abstract), keywords, main text, acknowledgements, references, tables, figures and captions to the table and figures. Each page of the manuscript should be numbered consecutively.

Submission of manuscript
Submissions on a diskette or compact disc (CD) are encouraged with the manuscript created on "Microsoft Word". It is required that the main text, list of references, tables and figures legends be stored in the text. Figures and pictures must be in Microsoft Word compatible software. The font used should be preferably be Times New Roman 12 pts. Author(s) must ensure that the content of the diskette and the hardcopy are identical.

The text for the manuscript should be in the following form:

Title page
A concise and informative full title including name(s), affiliation(s) and professional address(es) of the authors and the date of submission.

Abstract
The abstract should not be exceeded 250 words. The abstract should include the purpose of study, a brief description of the procedures employed, main findings and principal conclusions.

Keywords
A maximum of six keywords must be provided (in alphabetical order). Keywords need not repeat words used in the title.

References
References should be in alphabetical order. References in the text should be indicated by a figure within parenthesis. References to journals should be listed as follows: author's surname and initial, year of publication, title of paper, title of journal in italics, volume number in bold print, page number of the article.
For example

JournalArticles:
Dayre, M. & Girand, A. 1986. Mechanical Properties of Granodiorite from Laboratory. *Engineering Geology*, **23:** 109-124

Books:
Monson, R. R. 1980. *Occupational Epidemiology*. Boca Raton, Florida: CRC press.

Chapter in a book:
Taniguchi, N., Takagi, M. & Mikita, K. 1999. Microsatellite DNA Markers for Monitoring Genetic Change in Hatchery Stocks of Red Sea Bream (*Pagrus major*): a case study. In *Genetics in Sustainable Fisheries Management* (Mustafa, S., ed.), Oxford, UK: Fishing News Book (Blackwell Science): 206-218

Tables
Tables should be numbered according to their order of appearance in the text. Each table should be submitted on a separate sheet.

Figures
Drawings and photographs should be supplied in a format not smaller than the actual printing size and not larger than about twice this size. Good black and white, high contrast copies of drawings or glossy prints of photographs should be submitted. Do not send original art work. Lettering, scale-bars, symbols, and legends should be large enough to be readable after reduction to a format fitting page or column dimensions.

Captions
Captions of tables and figures should also be submitted on separate sheets.

Enquiries
In case of doubts, authors/ contributors may contact the Chief Editor.

All correspondence pertaining to the articles and journal subscriptions should be addressed to the Editorial Board at the following address:

BORNEO SCIENCE
School of Science and Technology
Universiti Malaysia Sabah
88999 Kota Kinabalu
SABAH, MALAYSIA
Tel. No: 6088-320000
Fax No: 6088-435324 / 6088-320174
e-mail: borneosc@ums.edu.my
hamami5253@gmail.com (Chief Editor)

BORNEO SCIENCE ORDER FORM

I am interested in ordering _____ copy/copies of Borneo Science.
My particulars are:

Name : _____

Position : _____

Organization : _____

Department : _____

Address : _____

_____

_____ Post Code/ Zip Code _____

Country : _____

E-mail : _____

Payment details :

☐ Please send me an invoice

☐ I am paying by Check/ Money Order No.

Check must be made payable to 'Bendahari UMS'

Signature : _____

Date : _____

Price	: RM 15.00
Student Price	: RM 12.00
Postal charges (in Malaysia)	: RM 1.50